BLIND MOTION IMAGE DEBLURRING USING CANNY EDGE DETECTOR WITH GENERATIVE ADVERSARIAL NETWORKS

IDRISS MOUSSA IDRISS

FACULTY OF COMPUTER SCIENCE AND
INFORMATION TECHNOLOGY
UNIVERSITY OF MALAYA
KUALA LUMPUR

2021

BLIND MOTION IMAGE DEBLURRING USING CANNY EDGE DETECTOR WITH GENERATIVE ADVERSARIAL NETWORKS

IDRISS MOUSSA IDRISS

DISSERTATION SUBMITTED IN PARTIAL FULFILMENT OF THE REQUIREMENTS FOR THE DEGREE OF MASTER OF COMPUTER SCIENCE (APPLIED COMPUTING)

FACULTY OF COMPUTER SCIENCE AND INFORMATION TECHNOLOGY
UNIVERSITY OF MALAYA
KUALA LUMPUR

2021

UNIVERSITY OF MALAYA

ORIGINAL LITERARY WORK DECLARATION

Name of Candidate: **Idriss Moussa Idriss**

Matric No: WOA170019/17036066

Name of Degree: Master of Computer Science (Applied Computing)

Title of Dissertation: Blind Motion Deblurring using Edge Detector with Generative Adversarial Networks

Field of Study: Image Processing

I do solemnly and sincerely declare that:

(1) I am the sole author/writer of this Work;
(2) This Work is original;
(3) Any use of any work in which copyright exists was done by way of fair dealing and for permitted purposes and any excerpt or extract from, or reference to or reproduction of any copyright work has been disclosed expressly and sufficiently and the title of the Work and its authorship have been acknowledged in this Work;
(4) I do not have any actual knowledge nor do I ought reasonably to know that the making of this work constitutes an infringement of any copyright work;
(5) I hereby assign all and every rights in the copyright to this Work to the University of Malaya ("UM"), who henceforth shall be owner of the copyright in this Work and that any reproduction or use in any form or by any means whatsoever is prohibited without the written consent of UM having been first had and obtained;
(6) I am fully aware that if in the course of making this Work, I have infringed any copyright whether intentionally or otherwise, I may be subject to legal action or any other action as may be determined by UM.

Candidate's Signature Date: 19 / 04 / 2021

Subscribed and solemnly declared before,

Supervisor's Signature

Name:

Designation:

BLIND MOTION IMAGE DEBLURRING USING CANNY EDGE DETECTOR WITH GENERATIVE ADVERSARIAL NETWORKS

ABSTRACT

Blind motion image deblurring has been investigated widely in recent years. Many methods and schemes have been proposed so far, with respect to edge-preserving. Edge information transfers the essential details of an image which is a primary factor impacting the visual effect. Edge-preserving is an important attribute during the process of image restoration. The main objective of deblurring is to generate a good approximation of the original image from the blurry image. However, blind motion deblurring has remained a challenging task for image processing and computer vision. Most of the existing algorithms rely on MAP (Maximum a Priori) and VB (Variational Bayesian) which are based on deterministic and stochastic methodologies, respectively, to estimate the blur function. MAP and VB both rely on particular assumptions to find the sources of the blur which make it difficult to use the edge-preserving treatment during the deblurring process. Therefore, including an edge-preserving treatment in the deblurring process would overcome these barriers as edges are the essential attribute of image information. This study proposes a combination approach of Canny edge detector with generative adversarial networks (GANs) to reconstruct the blurry image with edge-preserving without prior knowledge of the blurred image. The proposed method takes the blurred image with its detected edge, enhances it using Canny edge detector as an input, and produces a corresponding detected restored sharp edge with its image, evaluated by the GANs. Then the restored sharp image is compared against the ground truth (sharp) image. Experiments are conducted using the GoPro dataset. The proposed combined method has achieved good deblurring with edge-preserving results based on the evaluation metrics used.

Keywords: Blind Image Deblurring, Blind Motion Deblurring, Edge-Preserving, Generative Adversarial Networks (GANs), Canny Edge Detector.

[TITLE IN MALAY BAHASA]

ABSTRAK

Deblurring Gambar gerakan buta telah banyak disiasat dalam beberapa tahun kebelakangan ini. Banyak kaedah dan skema telah diusulkan sejauh ini, berkenaan dengan pemeliharaan tepi. Maklumat Edge memindahkan butiran penting gambar yang merupakan faktor utama yang mempengaruhi kesan visual. Edge-preserving adalah atribut penting semasa proses pemulihan imej. Objektif utama deblurring adalah untuk menghasilkan penghampiran gambar asal yang baik dari gambar yang kabur. Walau bagaimanapun, deblurring gerakan buta tetap menjadi tugas yang mencabar untuk pemprosesan imej dan penglihatan komputer. Sebilangan besar algoritma yang ada bergantung pada MAP (Maximum a Priori) dan VB (Variational Bayesian) yang masing-masing berdasarkan metodologi deterministik dan stokastik, untuk menganggarkan fungsi kabur. Kedua-dua MAP dan VB bergantung pada andaian tertentu untuk mencari sumber kabur yang menyukarkan penggunaan rawatan pemeliharaan tepi semasa proses deblurring. Oleh itu, termasuk rawatan pemeliharaan Edge dalam proses deblurring akan mengatasi halangan ini kerana tepi adalah sifat penting dari maklumat gambar. Kajian ini mencadangkan pendekatan gabungan pengesan tepi Canny dengan rangkaian lawan generatif (GAN) untuk membina semula gambar yang kabur dengan pemeliharaan tepi tanpa pengetahuan sebelumnya mengenai gambar kabur. Kaedah yang dicadangkan mengambil gambar kabur dengan tepi yang dikesan, memperbaikinya menggunakan pengesan tepi Canny sebagai input, dan menghasilkan tepi tajam yang dikesan yang sesuai dengan imejnya, yang dinilai oleh GANs. Kemudian gambar tajam yang dipulihkan dibandingkan dengan gambar kebenaran tanah (tajam). Eksperimen dijalankan menggunakan set data GoPro. Kaedah gabungan yang dicadangkan telah mencapai deblurring yang baik dengan hasil pemeliharaan tepi berdasarkan metrik penilaian yang digunakan.

ACKNOWLEDGEMENTS

Above all, all praises, appreciation, and thanks are to Allah Almighty, who has continuously blessed me with a lot of great people and opportunities in my life. I am very thankful and will never forget the teaching and guidance of my academic advisor, Associate Prof. Dr. Hamid Abdullah Jalab who has taught me two courses (Computer Graphics and 3D Animation Technology & Virtual Reality Concepts and Technology) which inspired my interests in the field of Image Processing and Computer Vision which enabled me to complete this research dissertation. Dr. Hamid has closely supported and guided me during my whole master's degree journey including defending my research proposal and master candidature, as well as the dissertation report.

I would like to reiterate my thanks and gratitude to the IsBD (Islamic Development Bank) scholarship program department for having granted me a master's student scholarship. Words cannot describe how much I owe my father Moussa Idriss Malloum for having had raised me and supported me from first day of my birth until the day he passed away when I was an undergraduate student in 2013. To my mom, Nassire Hassan Oumar, words can't describe how much I owe her as she has been the greatest mom any child could wish for. She has supported and educated all my other siblings by herself as a widowed woman. All that has made me into a courageous man to carry on fulfilling my dreams including this master's degree achievement. To my wife Kumba Sennaar, words can't describe how much I am deeply indebted to the unlimited support, help, love and assistance she has provided and for being there for me all the time, achieving this master's degree. To my older sisters Hawa and Kaltouma have inspired me and encouraged me to go beyond my limits by asking me each time we spoke, "how is your studying going" and "May Allah help you finish it with major success". I am very grateful for that. To my younger brothers Moukhtar, Hassan and Tarikh who have been very encouraging, loving and motivating, enabling me to get my master's degree completed, I am very thankful

for having you as my brothers. To my younger sisters Mariam and Izza as well as my orphan nephew Abakar's non-stop prayers for my success worked out for me and I am very grateful.

Finally, I would like to express my heartfelt appreciation to all my faculty members, classmates, housemates, relatives and friends for the wonderful support and guidance throughout this journey, I am indebted to the help you have provided to me.

TABLE OF CONTENTS

LIST OF FIGURES

LIST OF TABLES

LIST OF SYMBOLS AND ABBREVIATIONS

AM	:	Alternating Minimization
Averrage L_2	:	The distance of every model to the ground truth samples
BID	:	Blind Image Deconvolution/Deblurring
CNN	:	Convolutional Neural Network
dB	:	Decibel
e.g.	:	For Example
et al.	:	Et alibi
etc.	:	Etcetera
GANs	:	Generative Adversarial Networks
GPU	:	Graphical Processing Unit
IBD	:	Iterative Blind Deconvolution
i.e.	:	That is
IQM	:	Image Quality Measure
MAP	:	Maximum A posteriori
MATLAB	:	Matrix Laboratory
ML	:	Machine Learning
ML	:	Maximum Likelihood
MSE	:	Mean Square Error
MSSIM	:	Mean Structural Similarity Index
OpenCV	:	Open-Source Computer Vision Library
PSF	:	Point Spread Function
PSNR	:	Peak Signal to Noise Ratio
py.	:	Python

RAM	:	Random Access Memory
ReLU	:	Rectified Linear Unit
SSIM	:	Structural similarity index measure
TV	:	Total Variation
UQI	:	Universal Quality Index
VB	:	Variational Bayesian

CHAPTER 1: INTRODUCTION

1.1 Background

1.1.1 Importance of Images

In every aspect of human life, digital images have played a main role in the process of acquiring and sharing knowledge. They are produced by different digital imaging devices based on specifications and requirements. On one hand, there has been a technological revolution in digital imaging devices. As humanity has evolved, so has the need for high quality digital images for different digital applications such as security, TV, entertainment, medical imaging, astronomy, microscopy, law enforcement, etc. However, on the other hand these devices could produce potentially blurred images (Chang, Wu, & Tsai, 2017; Elmi Sola, Zargari, & Rahmani, 2018; Xiaonan Zhang, 2019) due to many reasons including motion blur which is the focus of this study. Motion blur may be caused by camera shake during the exposure time which considerably degrades the image's quality and leads to blurriness. It is the outcome of relative motion during the exposure time of the image between the camera and the scene. This includes both camera and scene objects in motion. Restoring these images from their degradation (blur and blindness) needs image deblurring methods since the primary purpose of the reconstruction is to estimate the degradation and use an inverse approach to recover the images from a blurry state. Therefore, image restoration is an ill-posed inverse problem due to the lack of or limited availability of prior information. As a result, image restoration solutions are rendered by either image deblurring or the blind image deconvolution techniques depending on the restoration problem (prior information) to be solved. Figure 1.1 shows examples of images when degraded (motion blind images) which makes impossible to notice all the information of the images.

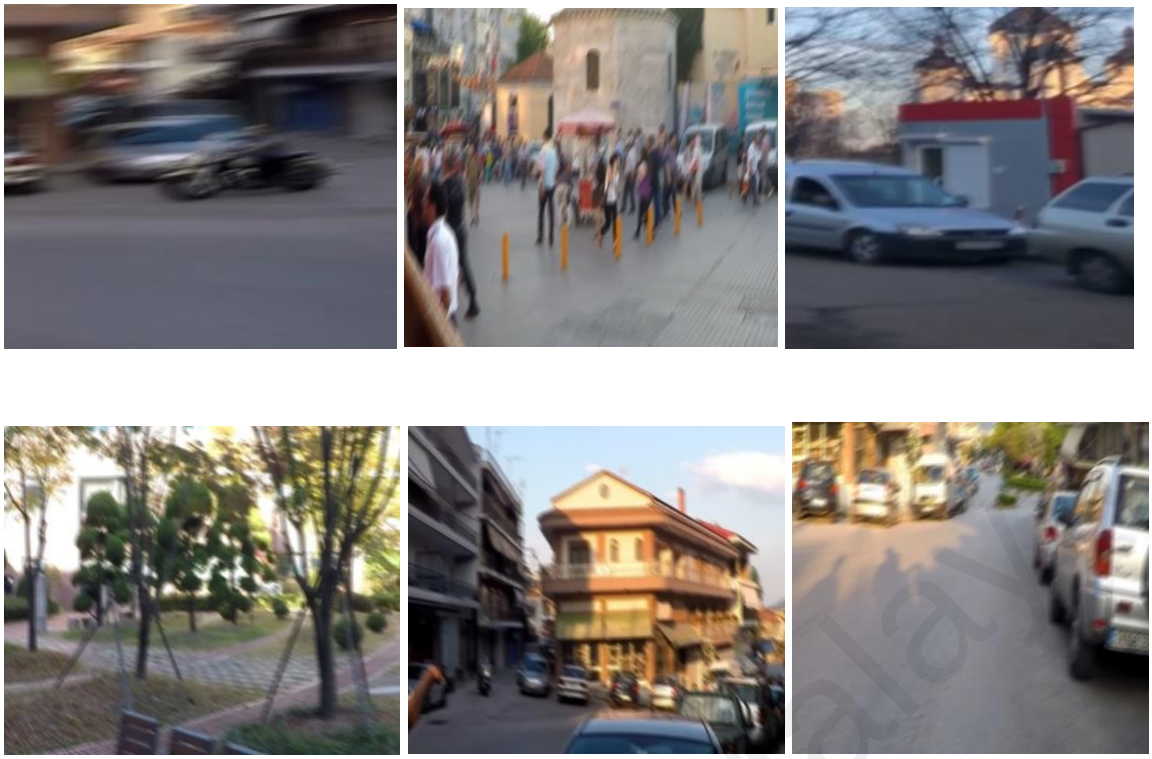

Figure 1.1: Examples of motion blind images

1.1.2 Deblurring Process

The main objective of the deblurring process is to generate a good approximation of the original image from the blurry image. The main objective of the deblurring process is to generate a acceptable approximation of the original image from the blurry image. The process is generally called a convolution filtering, deconvolution or deblurring. There are two deblurring methods: the non-blind and blind deblurring methods. The non-blind deblurring methods are concerned with estimating only the clear image which is the latent sharp image from the blurry image. In contrast, the blind deblurring methods involve estimating both the kernel blur which is the PSF (Point Spread Function) and the clear image (latent sharp image) from the blurry image (Chang et al., 2017; Elmi Sola et al., 2018; Gong et al., 2018; Xiaonan Zhang, 2019). The blind deblurring is one of the most difficult problems in image restoration since it is a severely ill-posed problem and solving it requires robust prior

information on the kernel blurs (PSF) and the clear image (latent sharp image). The prior information involves regularization techniques (Bai, Cheung, Liu, & Gao, 2019; Han & Kan, 2019; Ulyanov, Vedaldi, & Lempitsky, 2018) derived from deconvolution algorithms and other deep prior algorithms.

In fact, an efficient blind image deconvolution (image deblurring) technique must add an edge-preserving treatment during the deburring process for better feature extraction that can be used for different image manipulations and applications (Su et al., 2018).

Therefore, having a motion deblurring technique with more focused attention on edge-preserving contributes significantly to estimating the blur kernel and the clear image in both an efficient and effective way.

Over the years, there have been a variety of motion deblurring (blind image deconvolution) techniques with their respective restoration filters and regularization methods that have been proposed to recover the original images. Some of these techniques have less edge-aware / edge-preserving treatment regularization processes encompassed within the deblurring process while some do not. This number of schemes encompasses simultaneous and separate PSF (point spread function) estimation techniques, alternating iteration techniques, joint optimization techniques, time domain, frequency domain, etc. but can be distributed in the two existing groups of blind image deblurring methods including the maximum a posteriori (MAP) methods (Gong et al., 2018; Sada & Goyani, 2018; K. Zhang, Zuo, Gu, & Zhang, 2017) and the variational Bayesian (VB) methods(Dong, Pan, & Su, 2017) . Both MAP and VB are regularization approaches that are essentially mirror image in the two-dual world of deterministic and stochastic methodologies, respectively. But which of these methodologies best fits an efficient blind motion deblurring with edge preserving? Examples include the alternating iteration technique that is used to obtain a good approximation of the both the

kernel blur (PSF) and the clear image (latent sharp image) through ADMM (alternating direction method of multipliers) and half-quadratic penalty methods (Han & Kan, 2019) and blur kernel estimation based on the likelihood and the regularization for blur kernel and the clear image (Gong et al., 2018) which are classified under the MAP (maximum a posteriori) and VB (variational Bayesian) methodologies using deterministic and stochastic prior information, respectively with less or no focus on edge-preserving.

The current blind motion deblurring methodologies would be more robust and efficient if variational analysis in image and variational structure kernel are combined to help improve this gap. The focus of this research is to propose a combined approach for blind motion deblurring by using convolution neural network techniques to reconstruct the blurry image with edge preserving by estimating the kernel blur from the blurry image involving Generative Adversarial Network (Kupyn, Budzan, Mykhailych, Mishkin, & Matas, 2018; Xiaonan Zhang, 2019) and Canny edge detector filter (Thombare & Bagal, 2015; T. Wang, Zhang, Liu, Wiliem, & Lovell, 2019). Hence, the proposed method takes the blurred image with its detected edge evaluated using Canny edge detector as an input and produces a corresponding detected restore sharp edge with its image, enhanced by the GANs. Then the restore sharp image is compared against the ground truth (sharp) image. Experiments are conducted using dataset GoPro (Nah et al., 2017).

1.2 Problem Statement

Blind image deblurring is the problem of restoring an image from its degraded observation by estimating both the clear image and the blur kernel (PSF). Numerous regularization techniques involve the sparsity priors but that may generate the solution, producing the clear image and blur kernel same as the blurred image. The work proposed in the PhD dissertation by (Khan, 2014) analyzed both parametric and non-parametric forms of

PSF were treated for the blind deconvolution of images, but the latter deals with a much more complex blur shape that can't be easily modelled in the parametric form. Most of the current schemes/methods (Chang, Wu, & Tsai, 2017; Sada & Goyani, 2018) with different regularization techniques and types focus mainly on deblurring images degraded by non-parametric motion blurs (arbitrarily shaped motion blur PSFs) due to being more challenging. In their work (Dong et al., 2017) elaborated a blind image deblurring scheme which robustly estimated the blur kernel via salient edges and low rank prior. However, an edge-preserving treatment technique that takes into consideration both the clear image and the blur kernel during the deblurring process is needed. In addition, the support of the graphics processing unit (GPU) which is a result of the advancement of Computer hardware technology. As a result, big data, machine learning, deep learning, and image deblurring have made significant progress. Many researchers have proposed deblurring schemes that are applied to many applications, including medical imaging, traffic monitoring, blind motion image deburring, aerospace, target tracking and object recognition. Deblurring using generative adversarial networks (GANs) methods are used (Kupyn, Budzan, Mykhailych, Mishkin, & Matas, 2018; Xiaonan Zhang, Lv, Li, Liu, & Luo, 2019) by taking advantages of computing performance, although edge-preserving technique is less integrated. John. F Canny developed the Canny edge detection algorithm in 1986 and is an edge detection operator that uses a multiple-process algorithm to detect a wide range of edges in a noisy state of images (Krishnat B. Pawar, 2016; Preeti Topno, 2019; T. Wang, Zhang, Liu, Wiliem, & Lovell, 2019). Therefore, it can be used as edge-preserving filter with GAN to address Blind motion deblurring with Edge-Preserving, which solves the following limitations:

1. The loss of the blurred edge and details information during blind motion deblurring.
2. The noise artifacts are obvious during the BID process.

1.3 Research Questions

RQ1: What blind image deblurring (BID) regularization approaches and techniques are commonly used along edge-preserving treatment filter techniques?

RQ2: How to create a robust algorithm to remove the blur in image caused by camera shake and suppress the edge details?

RQ3: Can combining results from Canny edge detector filter with generative adversarial networks using CNN produce better blind motion image deblurring performance in terms of edge preserving?

1.4 Research Objectives

To investigate and propose a combined Blind motion deblurring scheme using Canny edge detector with generative adversarial networks (GANs) with edge-preserving, so that the deblurred images would be estimated based on the motion blur edges.

RO1: To investigate the existing blind image deblurring (BID) schemes presented in the relevant literature.

RO2: To propose a combination Canny edge detector with GANs algorithm for blind motion image deblurring to suppress the edge details.

RO3: To assess the efficacy of the proposed method with regards to its edge-preserving and compare it with other existing methods**.**

1.5 Research Scope

The research deals with Blind Motion Image Deblurring of noiseless images corrupted by motion blur. Blind motion is the outcome of relative motion in the exposure time of the image between the camera and the scene. The motion blur is shift invariant, where camera movement is only be parallel to the scene plane. This involves objects motion with both camera and scene. Images include both artificially blurred and real-life blurred images for blind motion. The scope of this research is limited to review the combined approach of Canny edge detector with generative adversarial networks (GANs)'s performance for blind motion deblurring with Edge-preserving. Other blind motions than due to camera and the scene exposure time are out of this scope of this study. The research focused solely on improving the edges-preserving during blind motion deblurring process. Blurs from an image that may be either inherent, or deblurring noise are not discussed in the analysis.

1.6 Research Significance

The research study is focused on providing blind motion restoration with edge-preserving solutions upon investigating and examining different blind image deblurring regularizations techniques and schemes. This will allow the various researchers in the field of computer vision and image processing to easily determine which blind motion deblurring with edge-preserving approach best suits their objectives based on the benefits and limitation of each approach. In fact, edges are important attribute to image information and preserving them with a special treatment would significantly make the work more efficient and effective. Thus, the research proposes a combination novel of the GANs and Canny edge detector filter to help result in a blind motion deblurring with edge-preserving.

1.7 Thesis Structure

The thesis organization is as follows.

Chapter 2 introduces the blind image deblurring problem and presents the findings of the literature review. The existing Blind Image deblurring regularization techniques and schemes are examined and for each, the blur kernel estimation, the achievement, and limitations are highlighted with focus on edge-preserving. Canny edge detector and generative adversarial networks algorithms are introduced. Edge preserving treatment in BID is reviewed.

Chapter 3 describes the entire research methodology of the proposed method. Full research methodology is explained. Initially, requirement analysis has been described and explanation of research design and implementation is fully detailed. The proposed method in this chapter consists of combining Canny edge detector with generative adversarial networks algorithms using deep convolution neural network are described and their algorithms and loss functions are expressed.

Chapter 4: This chapter presents major research results and also presents a detailed discussion of the core discoveries/outcomes of the research in comparison with findings of previous related studies. RQ3 of this research is answered in this chapter.

Chapter 5: This chapter gives the conclusive remarks about the overall study by giving an account of how the various research objectives were achieved, the major contributions and limitations of the research.

CHAPTER 2: LITERATURE REVIEW

2.1 Introduction

The field of blind image deblurring has spanned over a few decades and has applications in diverse fields including blind motion. There are many blind image deblurring regularizations techniques and methods that have been proposed so far. Although this problem has remained a challenging task for the image processing and computer vision research communities since the 1960s, a large range of statistical techniques and image processing approaches have been used. This chapter provides a summary of certain fundamental principles in the field of BID. The degradation model, various forms of motion blur and many techniques and methods of restoration are discussed including variational analysis in image, gradient prior, Variational Bayesian (VB), Maximum A Posteriori (MAP) regularization technique. Past literature encompassing BID related to motion blur with focus on Edge-preserving techniques is reviewed in depth.

2.2 Blind Image Deblurring

Blind motion deblurring algorithms are typically regarded as a type of blurring model that establishes the relationship between an imaging system's original and blurred images. The result of this process is the blurred image. Where the kernel blur is unknown, blind image deblurring is the method of restoring an image from its blurred state Therefore, blind image deblurring (BID) is an ill-posed inverse problem (Han & Kan, 2019; Sada & Goyani, 2018; H. Zhang, Li, Wu, & Zhang, 2020; Xiaonan Zhang et al., 2019). Selecting a method for blind image deblurring for camera-motion blur with edge-preserving can be accomplished through regularization and optimization techniques. There are many techniques and methods that have been proposed so far, although this problem has remained a challenging task for the

image processing and computer vision research communities. The primary issue stems from a lack of prior knowledge about the image. The blurring process may also result from a lack of optimal deblurring filters. The methods and techniques used include variational analysis in image, gradient prior, Bayesian variation, MAP regularization techniques (Elmi Sola, Zargari, & Rahmani, 2018; Ulyanov et al., 2018; H. Zhang et al., 2020). However, each of them may differ from one another in terms of robustness, computation time and edge-preserving due to the blind deblurring being parametric or non-parametric, uniform or non-uniform as well causes of blurring. Blind motion is one of the common degradations that can substantially degrade an image's quality. Different camera movements result in various blurs and it is important to distinguish the blurs when looking for a deblurring method which encompasses edge-preserving.

2.3 Mathematical Formulation

Typically, blind motion deblurring algorithms are based on a blurring model that defines the relationship between an original image and an imaging system's blurred images. A convolution between the input image and the transition degradation function arises from the distorted image. Estimation of the blur function is essential for image deblurring. In the captured image, any deficiency in the imaging system or environment can generate degradation. In order to describe the image development process, a linear system may be used. A captured image may concurrently be interpreted as the output of the Point Spread Function or the spatial impulse response convolution of the linear blurring system. Mathematically, the discrete form of the convolution (i.e. a spatially invariant stationary PSF), according to (Gultekin & Saranli, 2019; Kupyn et al., 2018; J. Wang, Lu, Wang, & Jia, 2012) is given by a stationary impulse response of the system across the image (i.e. a spatially invariant stationary PSF).

$$I_B = k * I_S + N \tag{2.1}$$

where I_B is the blurred image, k is the blurring kernel (known), I_S is the clear image or sharp latent image, * is the convolution operator and N is additive noise. If the blur kernel is given as a prior (known), recovering clear image is called a non-blind deconvolution problem or uniform blurring process, if the blur kernel is unknown, it is called a blind deconvolution problem which is modelled as non-uniform blur by:

$$I_B = k(M) * I_S + N, \tag{2.2}$$

where I_B is the blurred image, $k(M)$ are the unknown blur kernels calculated by the motion field M , I_S is the sharp latent image, $*$ denotes the convolution and N is an additive noise. Finding the blur function (the unknown blurred image I_B and the blur kernels $k(M)$) for each pixel is an ill-posed problem. Figure 2.1 illustrates the camera's blurring model. The frequency domain modeled by applying the Fourier Transform is given by,

$$I_B = k\ I_S + N \tag{2.3}$$

I_S = the scene (image) k = system's impulse response and I_B = the captured scene

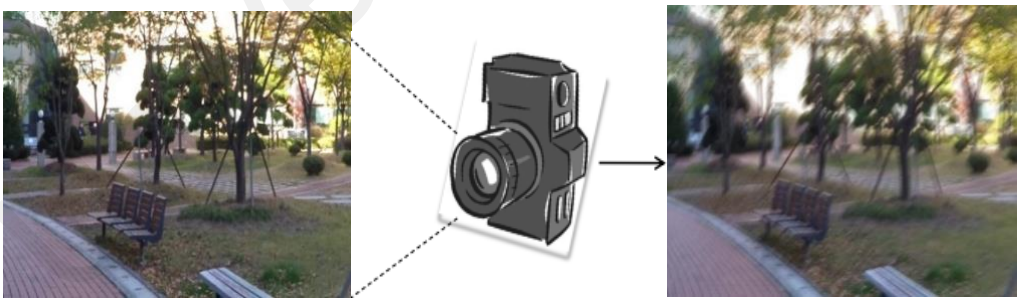

Figure 2.1: Image blurring model of a camera

The main objective of deblurring is to generate an effective approximation of the original image I_S'. Generally, this approach is known as convolution filtering or deconvolution (Dong et al., 2017; Han & Kan, 2019; H. Zhang et al., 2020) and known as deblurring when restoring

blurred images. In the case of noise free, which having prior knowledge of the $k(M) * I_S$, equation 2.3 can be used to find I_S', an approximation of I_S, by,

$$I_S' = k(M)^{-1} I_B \tag{2.4}$$

thus,

$$I_S' \approx I_S \tag{2.5}$$

This is considered inverse filtering (Gultekin & Saranli, 2019) . We can assume that the original signal can be accurately recovered if the exact parameters for the convoluting signal are identified.

Often, the method of inverse filtering is unsuccessful due to a lack of detail about the undesirable components of the signal. Figure 2.2 depicts an illustration of a restored blurred image using the deblurring model. The original image and the blurring kernel are both unknown. A general model of the image degradation / restoration process is given by Figure 2.3 as per (Rafael Gonzalez. , 2018).

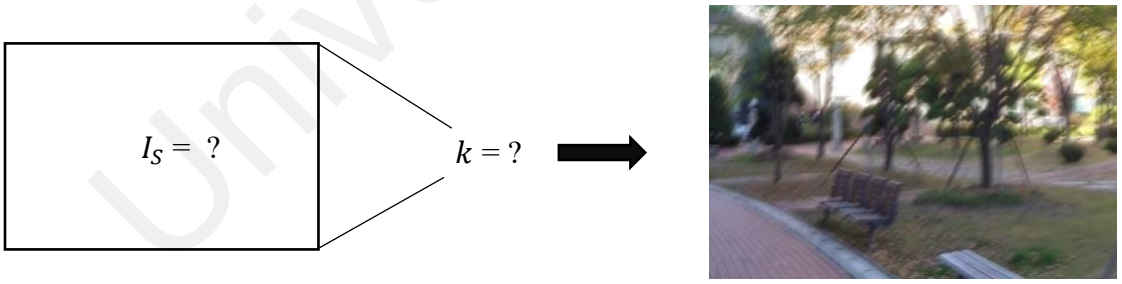

Figure 2.2: Deblurring model - The camera PSF knowledge and the scene are unavailable.

Inverse filtering provides an insufficient result in the case of the Fourier transform of the PSF holds zeros (Stockham, 1975).

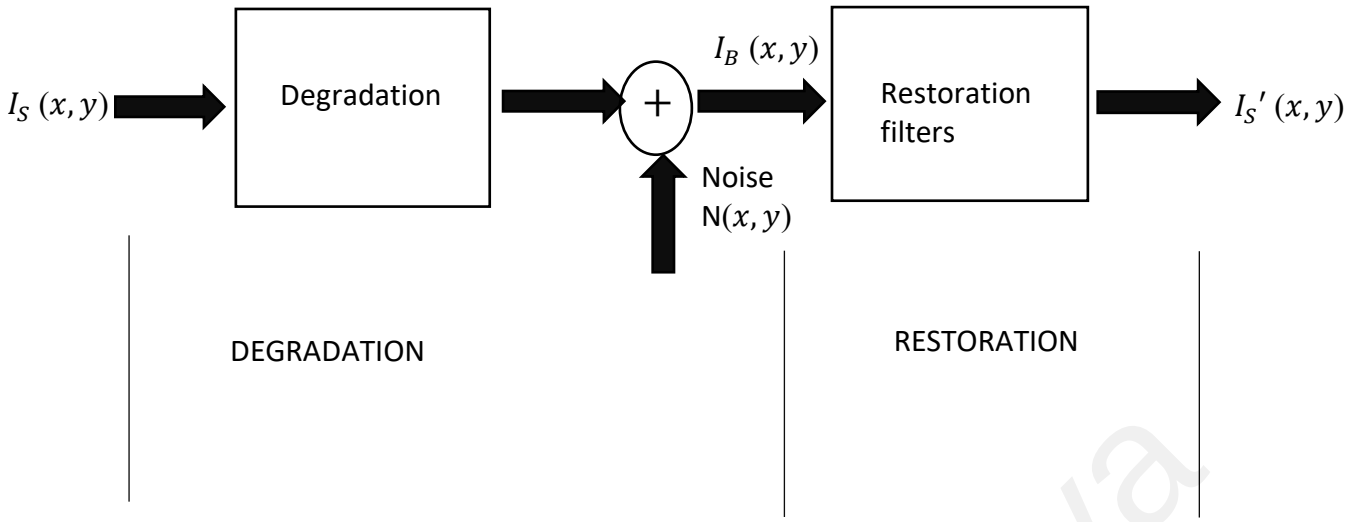

Figure 2.3: An image degradation model / restoration process

2.4 Blur Models

A selection of common blur types is described in the section below. Blurring functions are categorized in two main classes: space invariant (defocus) and space variant (motion) as per equation 2.6.

The space invariant is defined as a defocused blur arising from optical imaging devices. Image pixel location is independent of the general form of PSF. For each pixel location, the blurring function causes a uniform blurring effect during the convolution process.

The motion blur is defined as a space variant, resulting from the corresponding motion between the scene objects and camera. The blur kernel produces varying blurring effects depending on the image pixel location. Thus, different pixels produce different blurring effects.

$$I_B\,(x,y) = \int I_S(x-s, y-t)\; k(x-s, y-t; s, t)\,ds\,dt \qquad (2.6)$$

where I_S is the sharp image, k is the point-spread function (PSF) and I_B the blurred image. when PSF does not rely on the position (x, y) in the image, i.e., $k(x - s, y - t; s, t) = k(s, t)$, the integral transforms in convolution and hence it is space invariant PSF.

PSF can be divided into two groups, parametric and non-parametric based on its shape/form. In the parametric form, the PSF can be defined using a functional or parametric approach. An equation normally can be sufficient to generate the PSF.

Due to the complex shape of the PSF (non-parametric form) it cannot be defined using an equation based on its parameters. Images which have been destroyed by PSF are particularly challenging to deblur.

According to (Sorel & Flusser, 2008), most deblurring techniques were originally developed for handling space-invariant blurring PSF. Currently, space-invariant degradations are still considered a very challenging cause of blurriness

According to (Lagendijk & Biemond, 2009) the spatially continuous PSF $k(x, y)$ of any blur meets 3 restrictions, to be precise:

(i) the physics of the underlying image formation process, $k(x, y)$ can only take nonnegative values.

(ii) PSF $k(x, y)$ is also real-valued for real-valued images.

(iii) The failures in the image data are exhibited as passive operations on the data, meaning that no "energy" is consumed or produced. As a result, the PSF is constrained to satisfy for spatially continuous blurs:

$$\int_{-\infty}^{\infty} \int_{-\infty}^{\infty} k(x, y) dx\, dy = 1, \tag{2.7}$$

and for spatially discrete blurs:

$$\sum_{x_1=0}^{N-1} \sum_{x_2=0}^{M-1} k(x_1, x_2) = 1. \tag{2.8}$$

The perfect image convolution with a 2D PSF $k(x_1, x_2)$ is used to model the blurring of the input images.

2.4.1 Gaussian Blur

The Gaussian blur (or Gaussian smoothing) due to the image filtering by a low pass filter is estimated by a 2-D Gaussian function. A Gaussian function is used to calculate the transformation applied to each image pixel. Effect of this blur is denoted by a bell-shaped curve and is produced by a Gaussian filter. The blurring is dense in the center and fluffed at the edges as per the work of (El-Henawy, Amin, Ahmed, & Adel, 2018; Sada & Goyani, 2018). In addition, (Kupyn et al., 2018) used Gaussian filter in their motion blur kernel generation algorithm. The two dimension Gaussian filter over PSF, s and t, according to (Rafael Gonzalez. , 2018) is given as:

$$k(s, t) \frac{1}{2\pi\delta^2} e^{-(s^2 + t^2) * \frac{1}{2}\delta^2} \tag{2.9}$$

Equation 2.9 describes the PSF for atmospheric turbulence blur which is also considered a Gaussian blurring (Lagendijk & Biemond, 2009). Gaussian filter is among the techniques used to estimate blur kernel caused by different motion blur (i.e., defocus, camera shake, etc). Thus, Gaussian filter used by (Pan, Sun, Pfister, & Yang, 2016) to estimate blur length and angle, and then kernel estimated from these parameters for motion blur. Figure 2.4 displays the 15x15 Gaussian blur PSF and its related Optical Transfer Function (OTF). A Gaussian function is

either OTF or Fourier transform approximation of the Gaussian PSF. Figure 2.4(a) illustrates the impact of the blur due to atmospheric turbulence. Figure 2.5 (a) depicts a blurry video and Figure 2.5 (b) depicts a deblurred using atmospheric turbulence PSF estimation.

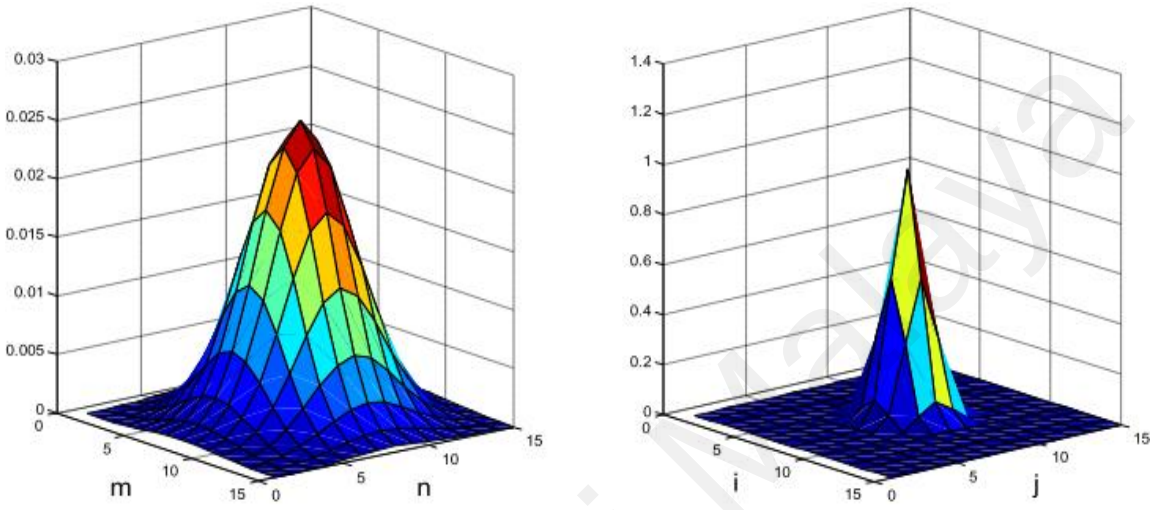

(a) (b)

Figure 2.4: Plot of a 15x15 Gaussian blur PSF with variance σ=2.5 (a) and its related plot frequency domain (b).

(a)

(b)

Figure 2.5: (a) Blurry video (b) Deblurred using atmospheric turbulence PSF estimation.

2.4.2 Motion Blur

Motion blur results from the corresponding motion between the recording system and the scene. The impact of motion blur is a motion based low pass filtering of the image data. High frequency information is often lost due to the filter. There are two main causes for motion: Camera vibration which affects all pixels in the image, and object motion which affects specific region in the image. The blurring affect can be described as a translation, a rotation, a sudden change of scale, or a combination thereof. However, a global translation is the most common case. The motion blur is a filter that causes an image to appear to be in motion by adding a blur in a specific direction. The motion is controlled by an angle (0 to 360 degree) or direction (-90 to 90) and by distance or intensity in pixels.

The Figure 2.6 (a) below illustrates the Fourier transform modulus of the kernel blur motion with L =7.5 and $\emptyset$ = 0. This figure shows that the blur is essentially a horizontal lowpass filtering process and that along characteristic lines, the blur has spectral zeros. These distinctive zero-patterns interline distance is nearly equivalent to N/L whereas Figure 2.6 (b) demonstrates the Fourier transform modulus for L =7.5 and $\emptyset = \pi/4$, respectively.

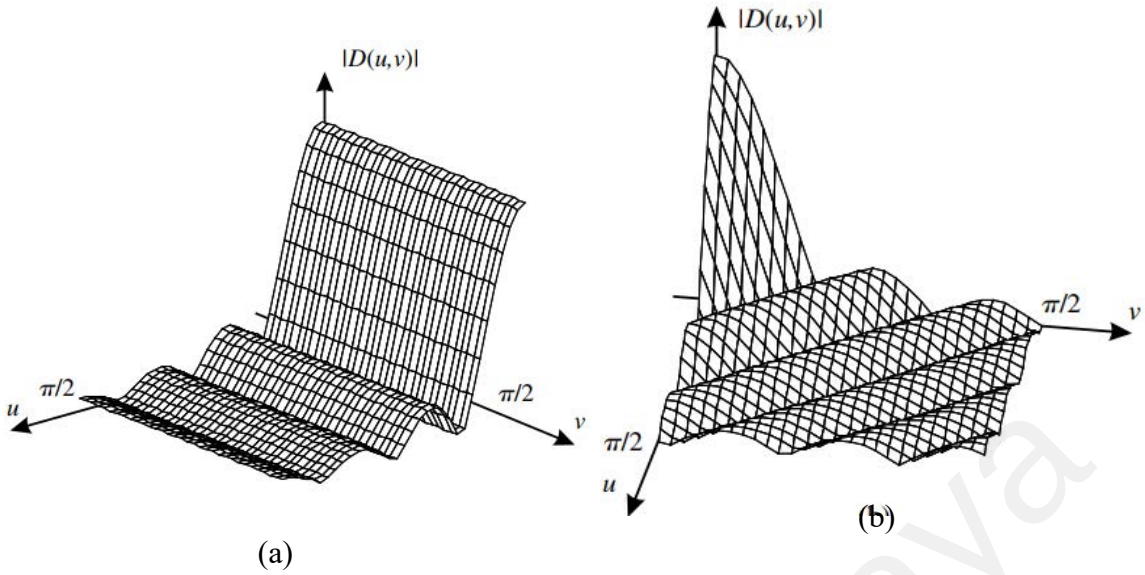

Figure 2.6: Kernel blur motion in the Fourier Transform, displaying $|D(u,v)|$for (a) L =7.5 and $\emptyset = 0$; (b) L =7.5 and $\emptyset = \pi/4$.

The blur is one-dimensional when the scene to be captured travels at a given speed proportional to the camera under an angle of $\emptyset$ radians with the horizontal axis across the exposure time. The motion length is denoted L and the angle is $\emptyset$, the PSF is given by equation 2.10 with reference to (Lagendijk & Biemond, 2009).

$$k(s,t;L,\emptyset) = \begin{cases} \frac{1}{L} \\ 0, elsewhere \end{cases} \quad if \sqrt{s^2 + t^2} \leq \frac{L}{2} \; and \; \frac{s}{t} = -\tan\emptyset \qquad (2.10)$$

where s and t are the PSF pixel coordinates.

Various methods have been suggested in the literature to remove motion blur. In order to remove motion blur during the capturing process, electro-mechanical stabilization techniques use actuators to cancel the relative motion between the image and the scene artifacts during the frame exposure process (Babak Rohani et al., 2014). The principal drawback of this approach,

though, is the difficulty of the control problem and the need for an additional structure. Another non-mechanical solution based on hardware manipulates the mechanism of image processing by configuring or manipulating the hardware of the camera. This provides the motion blurred images with properties that aid in the deblurring process. However, these techniques are usually based on motion blur induced by motion in the scene rather than camera motion.

For non-uniform motion blur images, (Chang et al., 2017) proposed a deblurring algorithm in which the blurred parts within an image are located and the blur amount of each edge is measured. A uniform focus map is then generated from these measurements. To obtain the PSF of each portion, the PSF of each blurred portion is estimated. All the portions and the corresponding PSFs are considered as inputs to a fast deconvolution algorithm in order to obtain the deblurred results. (Kupyn et al., 2018) use a free-kernel learning approach taking advantage of generative adversarial networks (GANs) to generate image pairs for training the color corresponding sharp and blurred images.

2.4.3 Camera Out-of-Focus Blur

An optical imaging system may cause Camera Out-of-Focus or Defocus blur. When an image captured by a camera takes a 3-D scene onto a 2-D imaging plane, certain parts of the scene are in focus while others are not. When the opening hole of the camera is circular, the Circle of Confusion (COC) occurs where the image of any point source is a small disk. The degree of defocus (diameter of the COC) is measured by the distance between the camera and object, the focal length and the aperture value of the lens. A reliable model encompasses both the diameter of the COC and the intensity distribution within it. A large degree of defocusing relative to the wavelengths requires a geometrical approach which results in a distribution of type uniform intensity within the COC. The spatially continuous out-of-focus blur of radius R,

with s and t are the PSF coordinates, is given by equation 2.11 with reference to (Lagendijk & Biemond, 2009)

$$k(s,t;R) = \begin{cases} \frac{1}{C\pi R^2} & if \quad \sqrt{s^2+t^2} \quad \leq \quad R^2 \\ 0, elsewehere \end{cases} \tag{2.11}$$

where C is a parameter chosen experimentally to satisfy the energy conservation law. Figure 2.7 shows the original PSF (a) and its spectral domain (b). The low pass behavior (in this case both horizontally and vertically) in Figure 2.7 (a), moreover, the characteristic pattern of spectral zeros in Figure 2.7 (b) as per (Khan, 2014).

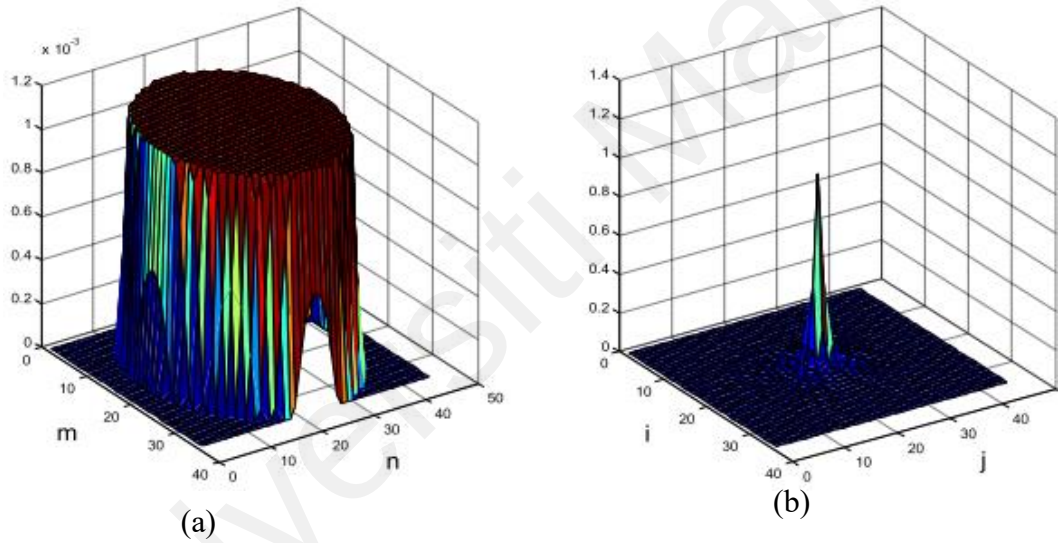

(a) (b)

Figure 2.7: Camera out-of-focus PSF plot for $R = 17$ (a) and its Fourier Transform (b)

2.5 Restoration methods and regularization techniques

In this section, the mathematical frameworks used to address BID including some classical restoration filters are discussed. The past and current blind image deblurring regularization techniques include: Maximum posteriori (MAP), Maximum Likelihood estimation (MLE), the Variational Bayesian (VB), Neural Networks and Generative Adversarial Networks (GANs).

These techniques use different estimation approaches to recover the clear quality image and the blur kernel throughout the blind deconvolution process. Whether based on deterministic or stochastic, the aforementioned regularization techniques are solutions to inverse and ill-posed problems in estimating the blur function. However, some may cause the edge-preserving treatment to be less integrated during the deblurring process.

2.5.1 Maximum A Posteriori (MAP)

Maximum A Posteriori (MAP) is a method for estimating some variable in the setting of probability distributions or graphical models. (Levin, Weiss, Durand, & Freeman, 2011) use a theoretical approach to study the advantages and limitations of the commonly used Maximum a Posterior (MAP) approach. In contrast (Perrone & Favaro, 2016) develop upon their study by focusing on Total-Variation (TV) regularization. In their work, (Shen, Xu, Zhang, Guo, & Jiang, 2019) utilizes the (MAP) method to construct the image prior and edge prediction. The method of estimating clear images can be formulated using MAP-based image deblurring methods as follows, according to (Han & Kan, 2019):

$$p(x, H|y) = \frac{p(y|x,H)\ p(x)\ p(H)}{p(y)} \tag{2.12}$$

where $p(x)$ and $p(H)$ are the probability density functions of clear quality image and blurring kernel. In image deblurring, $p(y)$ is known in advance, so equation 2.12 can be simplified as follows:

$$p(x, H|y) \propto p(y|x, H)\ p(x)\ p(H) \tag{2.13}$$

the priors on the blurring kernel, clear image and the likelihood term are represented by $p(y|x, H)$, $p(x)$ and $p(H)$

(Han & Kan, 2019) suggest a deblurring model based on MAP except that innovative local image edges are added, and the local edges are chosen from the bright and dark image channel, unlike conventional MAP-based techniques. The blur applied to the deblurring mechanism of the proposed procedure, however, is stationary, but the blurring kernels are often time-varying and space-varying in practical application, which is more complicated to estimate. In their work (Dong et al., 2017) propose an enhanced MAP in which kernel estimation is carried out through salient edges and low rank prior. The method could retain the salient structures and smooth the minor image gradient components, but if the blurred image includes a saturated field, it may not produce clear results. In practice, for blurred images with extreme noise, this is less effective.

2.5.2 Total Variational (TV) Regularization

Total Variation (TV) regularization is method used to prevent discontinuities in image processing. In the case of a known kernel k, I_S represents the true image, satisfying the relationship $I_B \approx k\, I_S$. Noise is denoted using the approximation symbol. According to (Chan & Wong, 1998) the predicted image I_S serves as the minimizer of a new functional with a goal of enforcing uniqueness and circumventing distortions as shown in equation. 2.12.

$$J_{TV}(I_S) = \frac{1}{2} \mid k - I_B \mid_2 \times^2 + \lambda\, TV(I_S), \tag{2.14}$$

where $J_{TV}(I_S)$ is a functional to be minimized and $\mid k - I_B \mid_2 \times^2$ is a fidelity (penalty) term and λ is value of TV. Total Variational (TV).

The main advantage of TV regularization is its ability to retain edge-preserving properties while removing texture fine-scale details. However, (Levin et al., 2011) note that total variation favors the no-blur solution over the true solution. In addition, in computer vision, computation

difficulties arise in the application of the TV-Norm when attempting to minimize the Laplacian of the latent image $J_{TV}(I_S)$ and distinguishing it from $J_{TV}(I_S)$ yielding the nonlinear equation proposed by (Estrela, Magalhaes, & Saotome, 2016):

$$T(I_S) = \nabla J_{TV}(I_S) = -\lambda\nabla\left(\frac{\nabla I_S}{|\nabla I_S|}\right) + k'(k\,I_S - I_B) = 0 \qquad (2.15)$$

The following computational problems emerge from the previous minimization:

The nature of the operator $\nabla\left(\frac{\nabla I_S}{|\nabla I_S|}\right)$ is highly nonlinear; and

$\nabla\left(\frac{\nabla I_S}{|\nabla I_S|}\right)$ and $k'k$ can be ill-conditioned can pose significant numerical challenges.

the Alternating Minimization (AM) method is discussed below:

AM Algorithm

1) Initial conditions: α , I_S' ϵ, k' and N, where ϵ is the error tolerance between estimates, k' is the initial estimate of k and N is the maximum number of iterations.

2) while ($n < N$) or (($I_S n$ - $I_S n$-1) < ϵ do

end

TV regularization is widely implemented due to its edge-preserving capabilities. Over the last two decades, research in this method has focused on application of higher order derivatives. (Estrela et al., 2016) conclude that improvement of TV regularization will depend on implementation of a differential operator that is more general in nature. This is due to the presence of a linear scheme and multiple inputs that improve versatility. In order to increase the efficiency of the regularization process, alternative algorithms that rely on dual variants of the TV norm standard will need more study in areas such as exponential spline wavelets or generalized Daubechies wavelets.

2.5.3 Variational Bayesian (VB)

Another successful strategy for overcoming BID problems has arisen from variational Bayesian (VB) inference. VB inference has led to the development of effective methods to recover consistent images from fuzzy observations, in tandem with other image models, such as Super Gaussian (SG) and Scale Mixture of Gaussian (SMG) representation. The model for image development for the BID Bayesian framework is defined as:

$$I_B = I_S \otimes k + n = K\, I_S + n, \tag{2.16}$$

where the detected blurred image is represented as $I_B \in \mathbf{R}^{\boldsymbol{N}}$ (a column vector of N pixels), $\otimes$ signifies the convolution operation, $I_S \in \mathbf{R}^{\boldsymbol{N}}$ is the original image which is unknown, $K \in \mathbf{R}^{\boldsymbol{N}\times\boldsymbol{N}}$ is the convolution matrix derived from the unknown blur kernel $k \in \mathbf{R}^{\boldsymbol{K}}$ and $n \in \mathbf{R}^{\boldsymbol{N}}$ is a noise term that is considered to be Gaussian with variance β^{-1}.

Considering the detected blurred image I_B, from a Bayesian viewpoint, the aim is to infer the latent (hidden) variables $z = \{ I_S , k\}$ and potentially the parameters of the model indicated by Ω. The model of image degradation in equation 2.16 can be written as follows as per (Ruiz, Zhou, Mateos, Molina, & Katsaggelos, 2015):

$$P(I_B|z, \beta) = N\,(I_B|K\, I_S, \beta^{-1}\mathrm{I}) \tag{2.17}$$

where β represents the observation model's precision parameter, and perhaps one of the parameters of the model to be estimated. It is important to provide detail on latent variables and detail on the model parameters. As a prior distribution $P(z|\Omega)$, which represents the info on z, and a prior $P(\Omega)$ on the model parameters, the Bayesian framework incorporates this necessary knowledge for the BID challenges.

The BID problem's global modeling can be formulated with these components as:

$$\text{as } P(z, \Omega, I_B) = P(I_B|z, \Omega)P(z|\Omega)P(\Omega). \tag{2.18}$$

VB methods are flexible and may be applied in image and in filter space. (Levin et al., 2011) express that the mixture-of-Gaussians (MOG) prior is more conducive to the filter space. (Xu, Zheng, & Jia, 2013) specify that for latent image estimation, using the image space formulation is more appropriate. In contrast, filter space formulation is more conducive to kernel estimation. However, additional work is needed to determine the most appropriate spaces for optimal image and kernel estimations. While noise is more amplified in the filter space, the image space appears to be less affected. In comparison to the image space, the filter space may be more computationally expensive. In fact, the total computation time in the filter space is approximately L times that of the image space, holding the number of iterations and L derivative filters constant.

2.5.4 Neural Networks (Learning based methods)

Neural networks are a learning based method developed for a non-linear mapping for image restoration while adapting parameters to training set. Primary techniques within neural networks used in BID are deep neural networks and convolution neural networks. Applying the neural networks for blind deblurring dates back to the last century. Recently, many types of neural networks have been used for various imaging problems (Ates, 2019; Lucas, Iliadis, Molina, & Katsaggelos, 2018) including blind motion deblurring. (Lucas et al., 2018), classify neural networks and describe DNN as a multilayer stack of simple modules. Each of these modules transforms its input into a new representation, which in turn serves as the input to the next module. In the deep-learning literature, modules are widely defined as layers, with each one containing multiple units or neurons. Figure 2.8(a) and Figure 2.8(b) illustrate their framework which is modelled in the equation 2.12. (Xu, Ren, Liu, & Jia, 2015) initiate convolution neural networks using large convolution kernels. (Ruomei & Ling, 2016) developed a combined approach using a classification network and regression network to

deblur images without prior information about the type of the blur kernel. (Ruomei & Ling, 2016) propose a pre-trained deep neural network (DNN) and a general regression neural network (GRNN) to initiate classification of the blur type and estimate its parameters. This approach combines DNN classification ability with the regression capabilities of GRNN. (Chakrabarti, 2016) employs a neural network application to predict Fourier transform coefficients of image patches in the frequency domain. Similarly, (Xiangyu, Jinshan, Yu-Jin, & Ming-Hsuan, 2018) utilize a CNN for edge enhancement prior to initiating kernel and image estimation. These techniques are often more effective than iterative optimization algorithms particularly in the case of linear motion kernels. However, the way in which they function is hard to interpret because their structures are often empirically determined.

$$y = T(x) + k, \tag{2.19}$$

where k represents the noise in the latent variables, y represents an observed signal as of the system output T, with input x. For example, x and y may denote two-dimensional (2-D) images, or x would consist of many video frames and y be a motion vector field, or x could represent a three-dimensional volume and y a set of 2-D (projection) images.

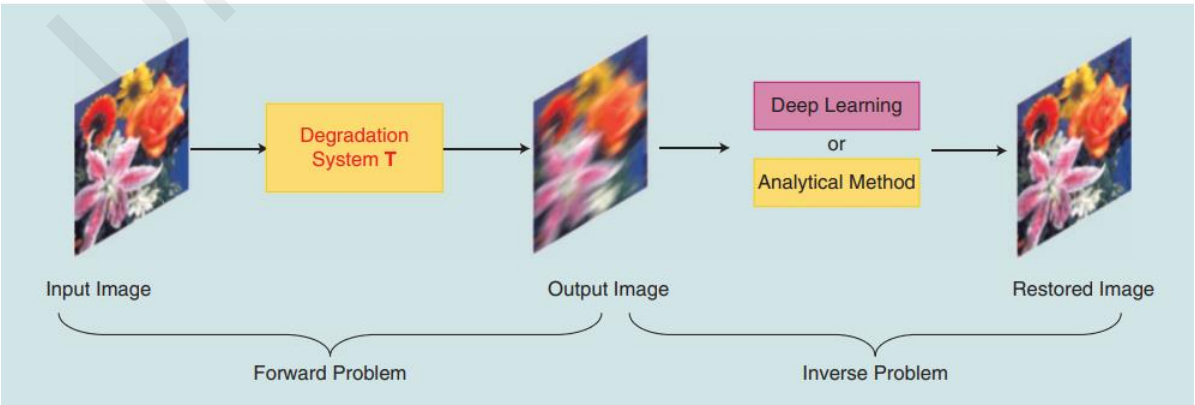

Figure 2.8: (a) The transformation T is added to an input image in a forward problem.

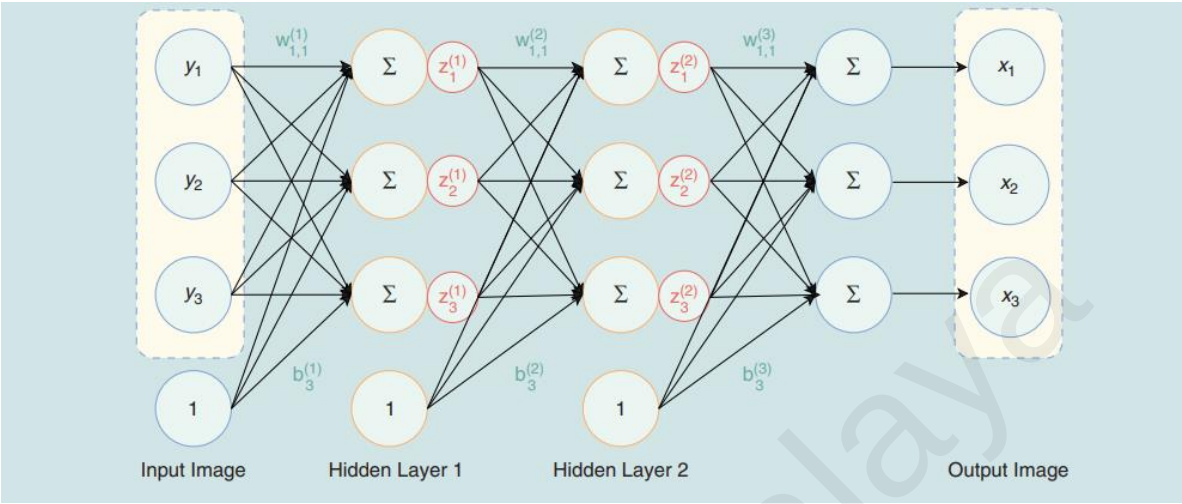

Figure 2.8: (b) A fully connected neural network with two hidden layers example.

The jth output neuron activation in layer I is defined as:

$$Z_j^I = f(\sum i\, W_{i,j}^I \times Z^{I-1}{}_i + b_j^I) \tag{2.20}$$

where $f()$ is the selected activation function. All weights W and biases b are learned during the training stage.

(Xu et al., 2015) propose a method for natural image deconvolution that does not rely on physical or mathematical characteristics. They offer a new way to construct a data-driven system using image samples that can be easily derived from online databases or directly from cameras. This is particularly useful because information on the cause of the visual artifacts is not needed to initiate the convolution neural networks and interpret the deconvolution operation. Unlike previous learning based methods, no pre-processing for image deblurring is required. However, the lack of the edge-preserving treatment throughout the deconvolution is

evident when evaluated using quantitative approach. (Xu et al., 2015) determine that the results of a comparison between the evaluation image set and deconvolution based on PSNRSs remain 28dB (Decibel).

2.6 Restoration filters

In the following section we describe some of the classical restoration filters that are currently used and studied in the field.

2.6.1 Inverse Filtering

Optimization of the deblurring process will require an estimation of the inverse of the PSF, which will be applied to the blurred image to recover the original image. According to (Rafael Gonzalez. , 2018), the inverse filtering can be applied directly in a noiseless blurred image. This has been identified as the simplest restoration approach, where an estimate $I_S'(x,\ y)$, of the transform of the original image is the result of dividing the transform of the degraded image, $I_B(x,\ y)$ by the degradation transfer function.

$$I_S'(x,\ y) = \frac{I_B(x,\ y)}{K(x,\ y)} \tag{2.21}$$

The division is elementwise, and in connection with

$$I_B(x,\ \ y) = K(x,\ y)I_S(x,\ y) + N(x,\ y) \tag{2.22}$$

Substituting the right side of the Fourier transform of the interference noise pattern in Figure 2.3 is given by the expression:

$$N(x,\ y) = K(x,\ y)I_B(x,\ y) \tag{2.23}$$

for $I_B(x,\ \ y)$ in equation 2.21 yields

$$I_S'(x,\ y) = I_S(x,\ y) + \frac{N(x,\ y)}{K(x,\ y)} \tag{2.24}$$

This expression concludes that the inverse Fourier transform of $I_S(x,\ y)$ cannot be recovered the undegraded image even if the degradation function be known. Furthermore, the ratio $\frac{N(x,\ y)}{K(x,\ y)}$ could easily dominate the term $I_S(x,\ y)$ if the degradation function is zero or has very small values.

For real blurred images, the kernel blur (PSF) is often not available. However, the PSF can be estimated under particular circumstances. (Xu et al., 2015) applied the blur kernel and its weight in the neural network model. By utilizing the singular value decomposition of the pseudo-inverse of their blur kernel, this allows them to initialize the weights of their large 1-D convolution kernels. This technique establishes a strong foundation for executing operation such as nonblind inverse filtering.

Inverse filtering requires two main components that are often difficult to obtain: the estimation of the degradation function and noise model details. In contrast, in blind deconvolution, accuracy is not emphasized and only an estimate of the degradation function is calculated.

The presence of noise amplification and the frequency of the domain zeros during the deblurring process inhibit accurate estimation of the correct coefficient values. The high pass quality of the inverse filter often introduces noise amplification during deblurring. Inaccurate filter estimation may lead to significant limitation and adverse effects due to the occurrence of frequency domain zeros in several deblurring images applications.

2.6.2 Wiener Filtering

The Wiener filter is named after Norbert Wiener who first proposed the concept in 1942. According to (Rafael Gonzalez. , 2018)Wiener filtering, , integrates the degradation function

and the statistical characteristics of noise into the image restoration process. This is distinct from inverse filtering, which considers the image and noise as random variables. Wiener filtering considers images and noise as random variables with the objective approximating (estimate) I_S' of the uncorrupted image I_S . It is important to note the mean square error between must be minimized. This error measure is defined as:

$$e^2 = E\{(I_S - I_S')^2\} \tag{2.25}$$

where $E\{\cdot\}$ is the estimated value of the argument. Wiener filtering considers 3 main assumptions: an uncorrelated relationship between noise and the image, either of these variables must have a mean of zero and the intensity levels in the estimated image are a linear function.

of those in the degraded image. According to these assumptions, the t frequency domain of error function of 2.25 is given in by the expression

$$I_S'(x,\ y) = \left[\frac{K'(x,\ y)S_{I_S}(x,\ y)}{S_{I_S}(x,\ y)\,|K\ (x,\ y)|^2\ + S_\eta(x,\ y)}\right] I_B(x,\ y) \tag{2.26}$$

$$= \left[\frac{K'(x,\ y)S_{I_S}(x,\ y)}{|K\ (x,\ y)|^2\ + \frac{S_\eta(x,\ y)}{S_{I_S}(x,\ y)}}\right] I_B(x,\ y)$$

$$= \left[\frac{1}{K(x,\ y)}\ \ \frac{K(x,\ y)^2}{|K\ (x,\ y)|^2\ + \frac{S_\eta(x,\ y)}{S_{I_S}(x,\ y)}}\right] I_B(x,\ y)$$

Some of the techniques employing Wiener filtering have been described by (Chokshi, Israni, & Chavda, 2016; Yang & Qin, 2016; Xinxin Zhang, Wang, Jiang, Wang, & Gao, 2016) to restore the latent image. However, each of these experiments produce varying results due to the initial causes of blurs.

(Chokshi et al., 2016) discussed the benefits and challenges of applying numerous image restoration approach such as blind and non-blind deblurring. The Wiener filtering techniques applied produce better quality image. The algorithm proposed by (Yang & Qin, 2016) uses non-blind image deblurring for motion blur. First, the blurred images are detected, and then the new blur classification algorithm proposes a way to

classify the blurred regions based on Wiener filtering. Finally, the structure of the kernel blur is determined. To remove spatially variant defocus blurs, (Xinxin Zhang et al., 2016) propose a single non-blind image deblurring algorithm based on the estimated kernel blur derived using Wiener filtering.

For optimal Wiener deconvolution, image frequency characteristics and adaptive noise details must be known. (El-Henawy et al., 2018) state that for blurred images caused by linear motion or unfocussed optics, Wiener filtering is most effective. This is due to the fact that this filter simultaneously inverts blurring and removes additive noise. Similarly, (Sada & Goyani, 2018) conclude that Wiener filtering delivers optimal results in the presence of Gaussian noise. While it is effective in terms of mean square error, it is less effective for PSNR measurement.

2.6.3 Iterative Blind Deconvolution Method

Implementation of the iterative Blind Deconvolution method employs deterministic constraints (non-negativity and finite support constraints) and leverages the capabilities of Fast Fourier Transform (FFT). The characteristics of PSP (Pressure-Sensitive Paint) filter heavily

influence the IBD scheme and provide the foundation of the single-shot measurement method proposed by (Pandey & Gregory, 2018). (Biemond, Reginald L. Lagendijk, & Mersereau, 1990) implemented iterative restoration techniques to remove linear blurs from images caused by pointwise nonlinearities such as film saturation and additive noise. They indicate that prior knowledge about removal of non-stationary blurs support the effective use of the iterative algorithms and discuss the convergence challenges. Furthermore, they conducted comparisons across various filters such as inverse filters, Wiener filters and pressure-sensitive paint which may be limiting solutions of variations of the iterations. The excessive noise magnification that is often associated with deblurring problems may be resulted using regularization. By terminating the algorithm after a specified amount of iterations, noise effects can be reduced. (Ayers & Dainty, 1988; Biemond et al., 1990) designed as depicted in Figure 2.9, the algorithm, incorporates the estimate of the image, the estimate of the PSF and the image in which has been degraded, which are denoted as $I_S{}'$, K' and I_B, respectively. The capital letters are the FFT versions of the corresponding signals. Lower case r indicates the iteration number of the algorithm. The procedure is encapsulated in the following manner:

1. The procedure is initiated with I_S as the input, a non-negative valued initial estimate.
2. Next, Fourier is converted to derive $I_S{}'r$ which proceeds with an inversion to construct an inverse filter. It is then utilized to produce a new estimate of I_B, $I_B{}'r$
3. The inverse Fourier Transform (iFFT) converts i_Br.
4. A positive constrained i_Br estimate is derived as a result of the introduction of image non-negativity constraints.
5. The spectrum of $I_B{}'r$ is derived from a Fournier transformation of i_Br.
6. An inverse filter is constructed from an inversion of the spectrum $I_B{}'r$ which then forms an estimation of IS'r by multiplying it by $K_r{}'$
7. $i_S{}'r$ is then formed from an inverse Fourier transformation of $I_S{}'r$.

8. A single iteration of the algorithm is complete following application of the image constraints to obtain the image $i_S{}'r$ estimate.

Repetition of the iterative loop is executed until two positive functions have been identified with the required convolution. Nevertheless, the IBD algorithm presents two primary obstacles:

- The ability to define the inverse filter is challenging in regions where the inverted function has low value regions.
- In $I_S{}'r$ and $I_B{}'r$, spectral zeros at frequencies offer no details about spatial frequency in process of image blurring.

The implementation of this scheme varies on the basis that the true image and PSF will render the entire deblurring procedure although the technique is common as a result of its minimal difficulty. Another benefit of this approach is its effectiveness with noise which is a commonly encountered challenged in BID.

(Pandey & Gregory, 2018) conclude that the iterative blind deconvolution algorithm is best suited for pressure-sensitive paint (PSP) and temperature-sensitive paint (TSP) data images. However, the researchers also conclude that is an effective option for meeting the deblurring requirements in the single-shot method where all other restoration algorithms have fallen short. This method appears to be a less robust for blurs which resulted from camera motion.

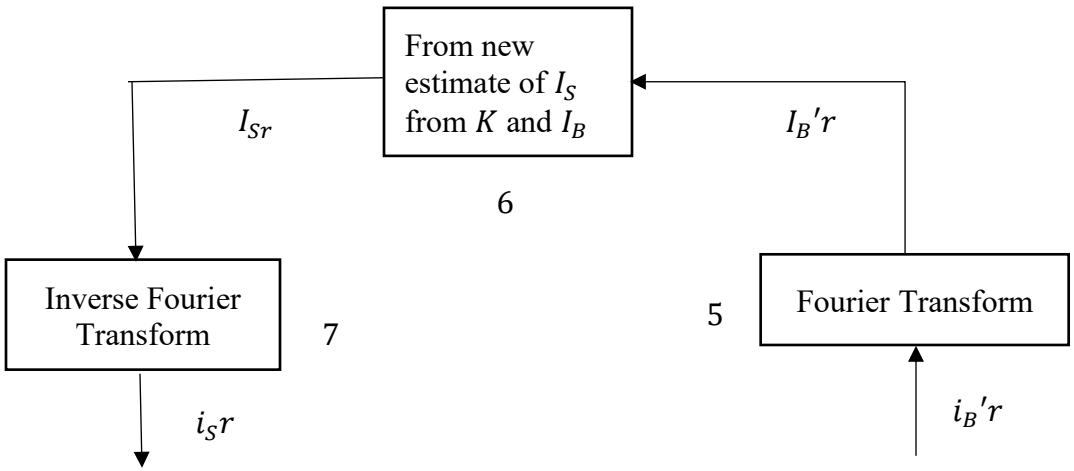

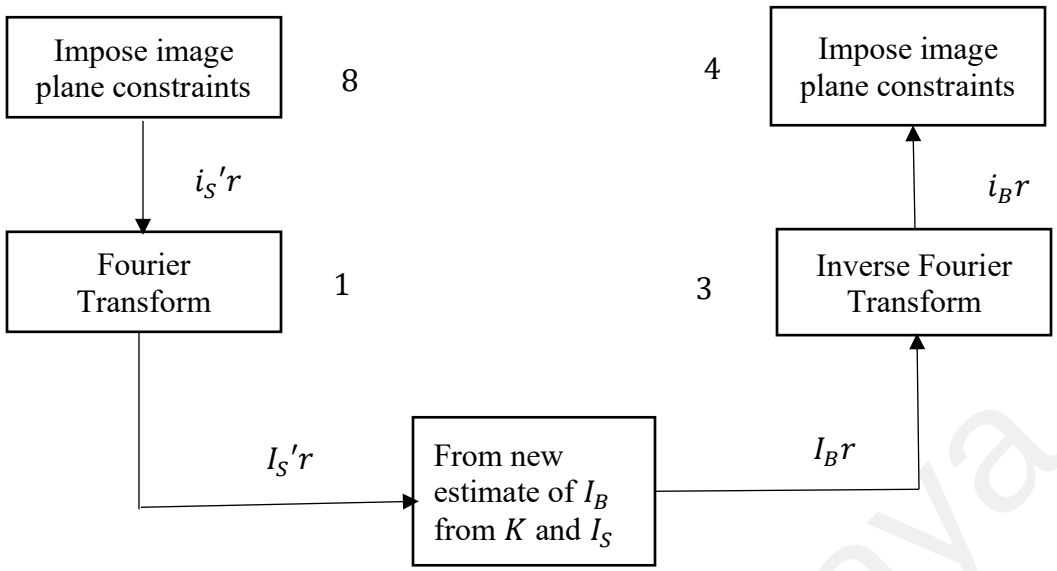

Figure 2.9: Block diagram of Iterative Blind Deconvolution (IBD) algorithm (Ayers & Dainty, 1988; Biemond et al., 1990).

2.6.4 Deconvolution using Richardson-Lucky Method

The LR was invented by Leon Lucy and William Richardson (Lucy, 1974; Richardson, 1972) and is designed to recover latent images blurred by a known PSF. While the PSF is known, knowledge about the noise is not available. A primary challenge of this method is the number of iterations required during the process. A very large amount of iterations will introduce ringing artifacts due to the slowness of the computational process. I_S , is denoted as the original image, the PSF K, I_B represents the degraded image and the iteration r, Bayes' theorem may be employed as follows according to (Richardson, 1972)

$$P(I_S|I_B r) = \frac{P(I_B r|I_S)P(I_S)}{\sum_{i,j} P(I_B r|I_S)P(I_S)} \tag{2.27}$$

Also considering $I_B r$ with respect to its dependence on I_S

$$P(I_S) = \sum_{i,j} P(I_S I_B r) = \sum_{i,j} P(I_S|I_B r)\, P(I_B r) \tag{2.28}$$

and

$$P(I_S|I_B r) = \frac{P(I_S|I_B r)}{P(I_B r)} \tag{2.29}$$

Substituting equation 2.27 in equation 2.28, we get

$$P(I_S|I_B r) = \sum_{i,j} \frac{P(I_B r|I_S)P(I_S)}{\sum_{i,j} P(I_B r|I_S)P(I_S)} P(I_B r) \tag{2.30}$$

$$P(I_S) = P(I_S) \sum_r \frac{P(I_B r|I_S)P(I_B r)}{\sum_{i,j} P(I_B r|I_S)P(I_S)} \tag{2.31}$$

The term $P(I_S)$ is also the desired term. An initial estimate of it was suggested using equation 2.27 which results in the iterative restoration method given in equation 2.32.

$$P_{r+1}(I_S) = P_r(I_S) \sum_r \frac{P(I_B r|I_S)P(I_B r)}{\sum_{i,j} P(I_B r|I_S)P(I_S)} \tag{2.32}$$

The LR algorithm requires an estimate of the support size of the kernel blur but is effective in reducing noise amplification. The algorithm is a solution for a non-blind deblurring process due to the prior knowledge obtained regarding the blurring kernel which is in the block-circulant matrix form.

2.6.5 Regularization Based Deblurring Algorithm

When only limited knowledge is available about noise, applying a regularization based deblurring algorithm is most effective. The convolution model of blurring is presented in equation 2.3 and using inverse filtering image estimates are shown in equation 2.33:

$$I'_S = \frac{I_B}{K} = I_S + \frac{N}{K} \tag{2.33}$$

The restoration error for this model is given by equation 2.26.

$$|I_S' - I_S| = \left|\frac{N}{K}\right| = \sqrt{\left|\frac{N}{K}\right|^2} \tag{2.34}$$

The restoration error has capacity for a large value resulting in amplification of high frequency noise (Lagendijk, Biemond, & Boekee, 1988). The system is depicted in equation 2.33 and shows where high frequency noise masks the desired solution I_S.

Regularization is often selected as a discrete Laplacian and is considered an estimation of a Wiener filter. However, the Wiener filter amplifies noise when the blurring filter is singular. The power spectrum estimation of the original image that is situated in the spatial domain are involved in the use of the regularized filter.

Using the standardized filter, the watermark image provides a prediction of the original image (Thongkor, Supasirisun, & Amornraksa, 2015). Embedded watermark images can be blindly recovered by detracting the predicted image from the image that is watermarked. Overall, better results are obtained from Wiener filtering compared to a regularized filter.

2.6.6 Deconvolution using Generative Adversarial Networks (GANs)

The graphics processing unit (GPU) is a result of the advancement of Computer hardware technology. As a result, big data, machine learning, deep learning, and image deblurring have made significant progress. generative adversarial networks (GANs) was developed by (Goodfellow et al., 2014) and is a class of machine leaning frameworks involving two competing neural networks (Generator and Discriminator). The process is initiated by the generator which generates images, and the discriminator must determine whether the image is real or not as shown in Figure 2.10. Although edge-preserving is less integrated, image deblurring using generative adversarial network (GANs) is widely used (Kupyn et al., 2018; Xiaonan Zhang et al., 2019). GANs algorithm is described below:

GAN Minibatch stochastic descent gradient training. A hyperparameter is the amount of steps to be applied to the discriminator, k. k=1

for number of training iterations **do**

for k steps **do**

Sample minibatch of m noise samples $\{z^{(1)}, \ldots, z^{(m)}\}$ from noise prior $p_g(z)$.

Sample minibatch of m noise samples $\{x^{(1)}, \ldots, x^{(m)}\}$ from data generating distribution $p_{data}(x)$

Proceed up the stochastic gradient to update the discriminator:

$$\Delta_{\emptyset_d} = \frac{1}{m} \sum_{i=0}^{m} [\log D(x^{(i)} + \log(1 - D(G(z^{(i)})))] \quad (2.35)$$

end for

Sample minibatch of m noise samples $\{z^{(1)}, \ldots, z^{(m)}\}$ from noise prior $p_g(z)$.

Proceed down the stochastic gradient to update the generator.

$$\Delta_{\emptyset_g} = \frac{1}{m} \sum_{i=0}^{m} \log(1 - D(G(z^{(i)}))) \quad (2.36)$$

end for

Any standard gradient-based learning rule may be used in the gradient-based updates.

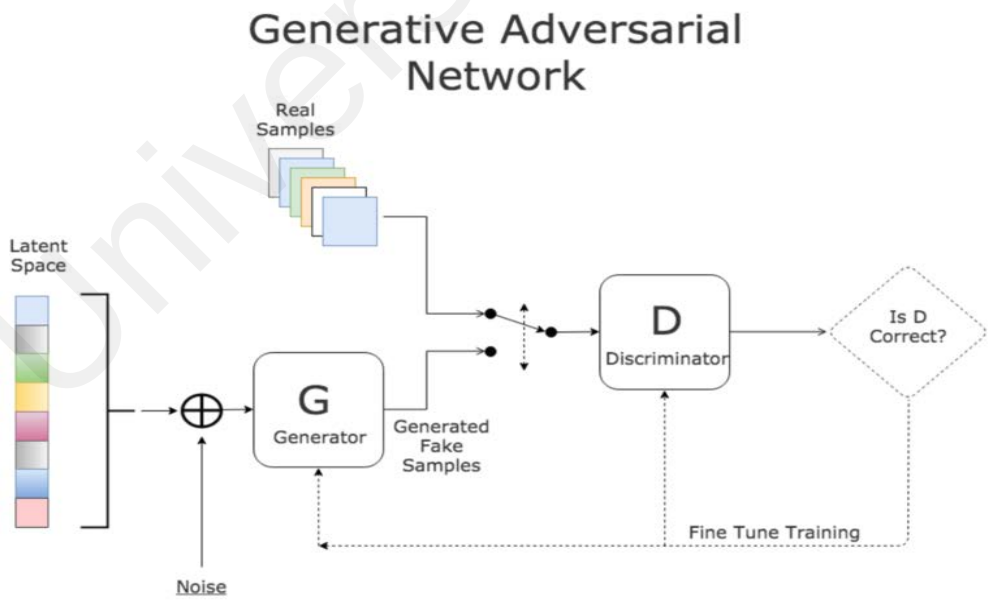

Figure 2.10 General building block of GANs

In their work (Kupyn et al., 2018), they describe DeblurGAN as an end-to-end learned method for motion deblurring. The conditional GANs and associated content loss form the foundation for DeblurGAN learning. A realistic dataset is possible as per the novel method proposed by the authors to generate synthetic motion blurred images from sharp ones. Although edge-preserving is not maintained throughout the deconvolution process, these results are effective in obtaining sharp images from blurred images. In addition, GANs is also a solution used for edge detection (Zeng, Yu, & Wong, 2018). In fact, implementing an edge detection algorithm provides better results than a simple image deblurring process with edge-preserving.

2.6.7 Canny Edge Detector Filter

John. F Canny in 1986 developed the Canny edge detection algorithm in 1986. The Canny operator follows a multiple-steps process. Initially, a Gaussian convolution of the image is implemented to smooth it. Next, in order to underline image regions, a simple 2-D first derivative operator is applied. The ridges found in the gradient magnitude image are caused by the edges around the image. Non-maximal suppression is initiated when the algorithm follows a track across the ridges. The algorithm sets all the pixels that are not located on the ridges to zero which provides a thin line in the output.

$$\text{Edge\_Gradient (G)} = \sqrt{G_x^2 + G_y^2} \quad (2.37)$$

$$\text{Angle } (\emptyset) = \tan^{-1}\left(\frac{G_x^2}{G_y^2}\right) \quad (2.38)$$

The Canny edge detector filter is effective in solving certain image processing, computer vision and computer graphics challenges involving edge detection, edge-preserving and disentanglement. For example, (T. Wang et al., 2019) combine Canny edge detector with generative adversarial networks (CANNYGAN) for Edge-Preserving image translation with

disentangled Features. Similarly, (Mane & Pawar, 2014) use Canny edge detector techniques to deblur blind images using blind deconvolution. Their utilization of BID is limited to Gaussian blurs and is based on maximum likelihood estimation algorithm (MAP). To determine the effectiveness of edge detection techniques (Thombare & Bagal, 2015) compare Canny edge detector filter with other methods. The Canny edge detection algorithm can detect the local statistical distribution of image gradient values in a block so that edges in low contrast regions can be detected.

2.7 Edge-Preserving in BID

Including edge-preserving in the blind image deblurring process is essential for image information, manipulation and is currently used in computer vision, image processing and image analysis applications. In the image formation process, edges are an important element, particularly for extraction and other manipulation techniques. Edge-preserving operators are widely used in image processing, computer vision and computer graphics applications (Hanika, Dammertz, & Lensch, 2011). (Su et al., 2018) categorized the edge-preserving techniques in two classes: Weighted average filters (explicit/implicit) and non-average filters. Both classes are effective for BID with edge-preserving.

2.8 Review of Blind Motion Image deblurring techniques

Blind motion image deblurring is a process of estimating both the true image and the kernel blur using partial information available/deduced from the blurred image and an interpretation of the blurring system's characteristics. It is not a new concept, and the abovementioned approaches and regularization techniques to solving the problem have been suggested, depending on the type of degradation and image models (Chakrabarti, 2016; El-Henawy et al., 2018; Sada & Goyani, 2018; H. Zhang et al., 2020) and the edge-preserving parameter applied

during the deblurring process. These methods span the spatial to spectral domains, are parametric or non-parametric, and are adaptive to batch processing. Such examples are the Maximum A Posteriori (MAP) (Han & Kan, 2019), Richardson-Lucy method, Total Variation (Estrela et al., 2016) and Maximum Likelihood (ML) method. Although these methods provide some solutions to the BID problems, many of them fall short in terms of robustness, computational performance, and the restored image quality. When restoring blind motion images, the robustness of these schemes remains or becomes questionable. As a result, BID learning-based methods are more efficient when come to robustness and image restoration quality although edge-preserving still remains a challenging task during the deblurring process.

Neural networks are a type of learning based method for evaluating a non-linear mapping for image restoration when adjusting parameters based on a training set. Deep neural networks and convolutional neural networks are the two main neural network methods used in BID (Chakrabarti, 2016; Lucas et al., 2018; Xiangyu et al., 2018). Thus, choosing a learning based method to restore image blurs caused by camera motion would be more efficient and result in images of a higher value of PSNR despite edge-preserving challenges. In fact, there are many different schemes made up of different CNNs which have been used to solve blind motion image deblurring problems. Examples include Generative Adversarial Networks (Goodfellow et al., 2014; Kupyn et al., 2018; Xiaonan Zhang et al., 2019) which produce better results in terms of image quality in addition to robustness and computational efficiency.

Edges transfer important information about images and are a crucial aspect impacting the visual outcome. Finding a filter to first detect and enhance the edges during the deblurring process is desperately needed. As a result, Canny Edge Detector (Bagal, 2015; T. Wang et al., 2019; Yuan & Xu, 2015) would be an efficient candidate filter to detect the edges of the blurred image and enhance it throughout the deblurring process. In order to smooth out the images

efficiently, the Canny edge operator is still not enough. Taking the improved Gaussian filter into consideration, the adaptive parameters for local image variance and minimum variance to make the edge detection (T. Wang et al., 2019) and smoothing more adequate, accordingly. Thus, the research study proposes combining Canny edge detector filter + Generative Adversarial Networks (GANs) to recover a blind motion image with more focus on edge-preserving and production of good quality images.

2.9 Summary

In this chapter, we introduced the topic BID with a focus on the restoration methods, regularization techniques and restoration filters used in this research. Restoration methods and regularization techniques discussed include maximum a posteriori (MAP), total variation (TV), variational bayes (VB) and neural networks (learning based methods). BID Filter techniques discussed include inverse, Wiener, GANs, Canny edge detector, Richardson-Lucky, iterative, and regularized based filters. A critical analysis of the existing BID techniques in the literature was provided and schemes relevant to the research were reviewed.

CHAPTER 3: RESEARCH METHODOLOGY

3.1 Introduction

This chapter presents the complete methodology of the proposed blind motion image deblurring using Canny edge detector with generative adversarial networks scheme. The chapter is divided into two sections for better explanation of the proposed method. First, the analysis of the research requirements is explained. Secondly, a brief description of the research design and implementation is described. The proposed method consists of combining Canny edge detector filter + GANs to recover a blind motion image with edge-preserving. The method structure comprises a Canny edge detector + generator and discriminator with a trio path network. This chapter proceeds with the following sections: brief discussion of research requirement analysis, general structure of the proposed algorithm, the specific and complete research design and implementation, and summary.

3.2 Research Requirement Analysis

Requirement analysis is initiated and followed by the development of the proposed method. Adequate analysis of the research requirements will make the blind motion image deblurring method proceed smoothly. Figure 3.1 provides an illustration of this process.

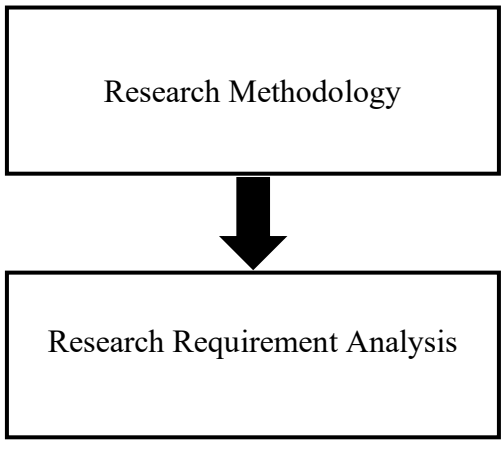

Figure 3.1: Research methodology phase

Evaluation of existing methods and selecting a suitable scope to develop the proposed method proceed as follows:

i. Existing methods review and comparison.

This step is fundamental in the proposed method for this research. Related research literature is reviewed, and an in-depth analysis is conducted to explore issues of the existing blind motion image deblurring methods. In chapter 2, a brief review of existing literature helped to identify the problem statement and helped set the research objectives accordingly. Moreover, analysis of drawbacks, limitations and advantages of existing literature helped to set the research aim.

ii. Selecting the scope to develop the proposed blind motion image deblurring using Canny edge detector with generative adversarial networks method.

A comprehensive literature review is completed to select the scope of this research and the structure of the proposed scheme. Canny edge detector + generative adversarial networks are combined using CNN for its outstanding performance in representing a high-level semantic, to train and test the data in this study. Three network channels are developed in the training set for the process: The canny edge detector + the two GANs neural networks, the generator, and discriminator. The training set takes the blurred image with its detected edge evaluated using Canny edge detector as an input and produces a corresponding restored sharp edge with its image, enhanced by Canny edge detector. Then the restored sharp image is compared against the ground truth (sharp) image by GANs.

3.2.1 Image Dataset

In their work (Nah, Kim, & Lee, 2017), they developed the GoPro dataset using images taken by a GOPRO4 Hero Black camera. The dataset contains 3214 pairs of images that are blurry and sharp at 1280x720 resolution. The researchers recorded latent image details and integrated this information over time for blur image generation. This is different from

the standard kernel modeling to convolve a latent image. The blurry image is generated when there is an accumulation of sharp image stimulation during exposure as light enters the camera sensor. The user GOPRO dataset is publicly available at https://github.com/SeungjunNah/DeepDeblur_ release. Sample of images are shown in Figure 3.2.

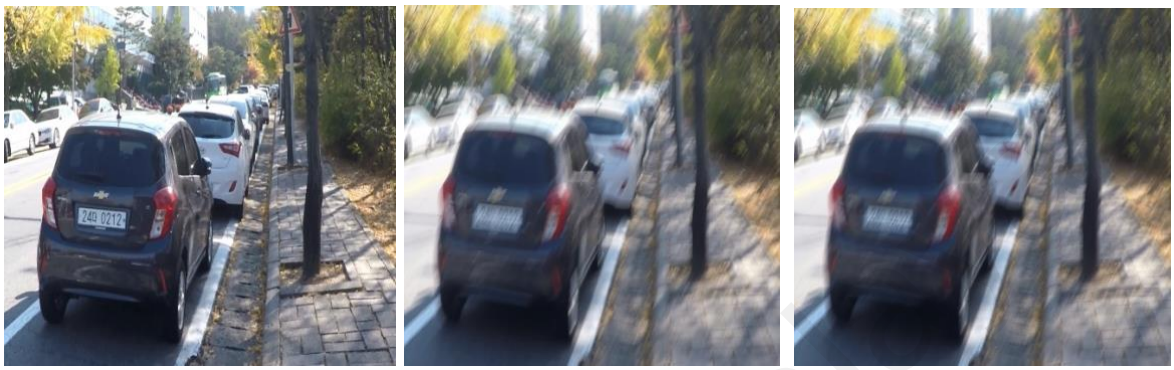

(a) (b) (c)

Figure 3.2 Sample of images. (a) Ground truth image. (b) Blurry image generated by convolving a uniform blur kernel. (c) Blurry image by averaging sharp frames.

3.3 General Structure of the Proposed method

This section presents the main structural design of the proposed blind motion image deblurring using Canny edge detector with generative adversarial networks method using CNN and explains the full implementation phase. The following section will explain the full steps of the proposed method as per Figure 3.3.

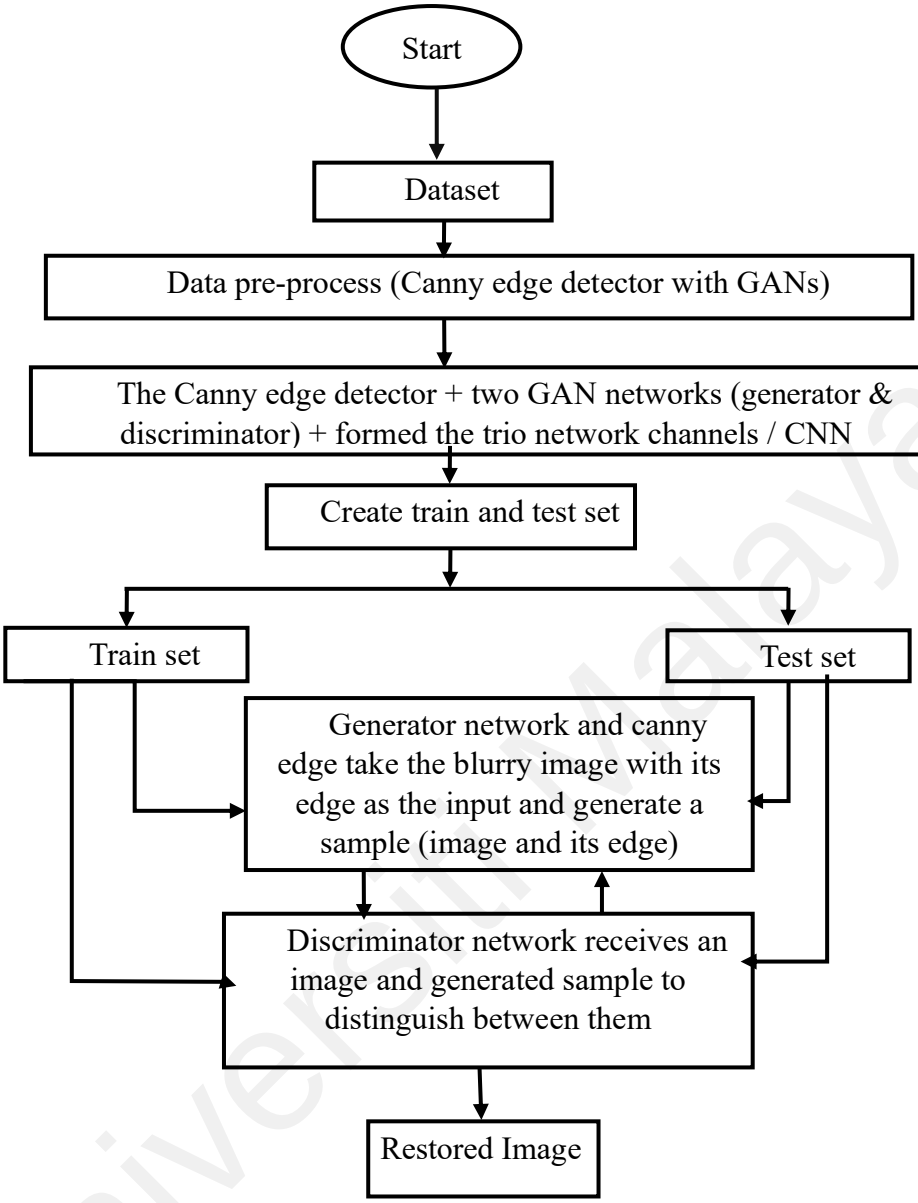

Figure 3.3: Research Design structure

3.4 Design and Implementation

The method structure consists of Canny edge detector + generator and discriminator with a trio path network. The role of the edge detector is to predict the edge of the blurred image, evaluate, enhance, and forward it to GANs. The generator network is responsible for rotating image features on multiple acceptance scales and developing a novel synthetic image by

tricking the discriminator network into believing it has received a real image (the blurred edge and the enhanced restored sharp edge). In order to help the network, create sharper images, the model incorporate the edge info created by the Canny edge detector.

3.4.1 Generator and Discriminator deblurring training

The blurred image is utilized as the input by the generator network, then the discriminator network will attempt to distinguish between the restored and sharp images as per the Figure 3.4.

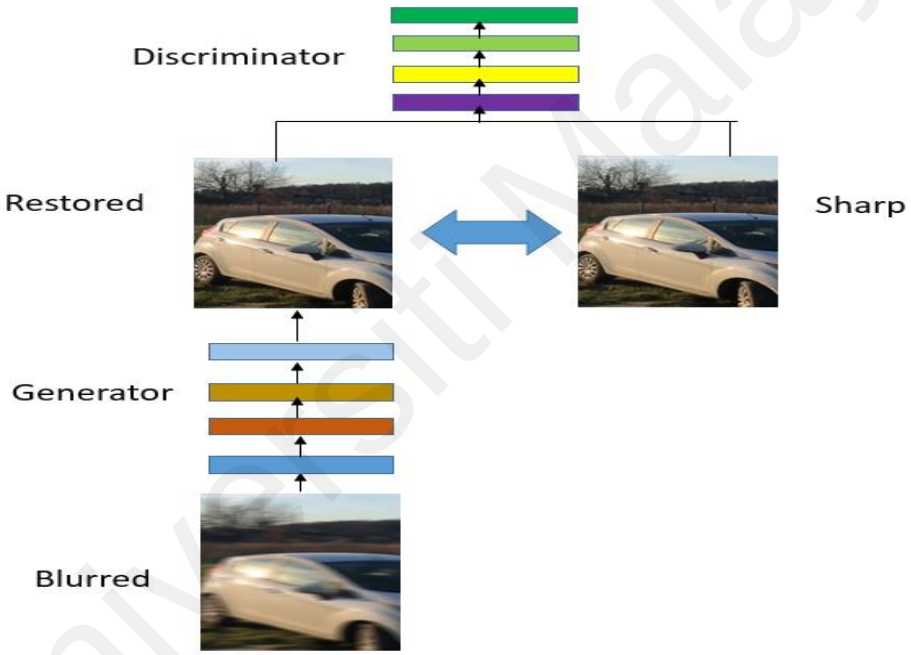

Figure 3.4: Generator and Discriminator deblurring training

The discriminator network takes the restored and sharp images and calculates the distance between them. Figure 3.5 depicts the Canny edge detector + GANs Architecture through the deblurring process using CNN.

3.4.2 The CNN Architecture of GANs +Canny Edge Detector

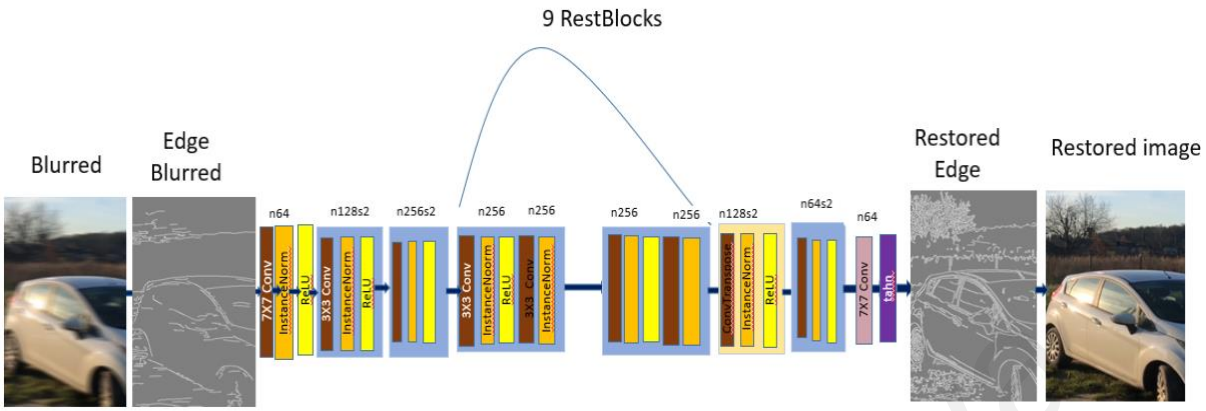

Figure 3.5: Architecture Canny edge detector + GANs through the deblurring process using CNN

(He, Zhang, Ren, & Sun, 2015) proposed the model which is comprised of two strides CNN with stride ½, 9 residual blocks and 2 transposed convolution blocks. Each ResBlock contains two specific layers (convolution and instance normalization) and a ReLU activation as shown in Figure 3.5.

3.4.3 Canny Edge Detector

The original blurred image edges are extracted, and texture details are gathered by the Canny edge detector using open CV algorithm as per Figure 3.6 below.

The original Canny algorithm involves the following steps:

i. Image smoothing

As per the equation 2.1,

$$I_B(x, y) = K(x, y) * I_S(x, y) \tag{3.1}$$

$I_S(x, y)$ is output smoothed image.

ii. Calculation of the Image gradient

The convolving image $I_S(x, y)$ with partial derivatives of a 2-D Gaussian function is calculated using each pixel location where the horizontal and vertical gradients $K_x\ (x, y)$ and $K_y\ (x, y)$ appear.

$$K(x, y) = \frac{1}{2\pi\sigma^2}\, exp\left[\frac{x^2+y^2}{2\sigma^2}\right] \tag{3.2}$$

iii. Gradient magnitude and direction

The gradient magnitude $M(x, y)$ and direction $\theta_G(x, y)$ at every pixel location is evaluated as

$$M(x, y) = \sqrt{K_{x^2}\ (x, y) + K_{y^2}\ (x, y)} \tag{3.3}$$

$$\theta_G(x, y) = \arctan\left(\frac{K_y\ (x,y)}{K_x\ (x,y)}\right) \tag{3.4}$$

iv. Non-maximum suppression (NMS)

v. Low and high threshold

Based on the histogram magnitudes of the entire image gradients, it measures low and high thresholds.

vi. Hysteresis thresholding.

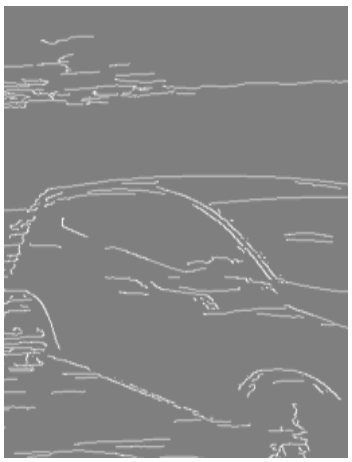

Figure 3.6: Canny Edge Detection

3.4.4 Motion Blur Kernel generation algorithm

In this research method, the work done by (Kupyn et al., 2018) is adopted in this research for the Motion Blur Kernel generation algorithm as described below:

Parameters:

M = 2000 – iterations number,

L_{max} = 60 – movement max length,

p_s = 0.001 – probability number of the impulsive shake,

I – inertia number from (0,0.7),

p_b – big shake probability, uniform from (0,0.2),

p_g – probability of Gaussian shake, uniform from (0,0.7),

φ – initial angle, uniform from (0,2π),

x – trajectory vector.

1: **procedure B**LUR(Img, M, L_{max}, p_s)

2: $v_0 \leftarrow \cos(\phi) + \sin(\phi) * i$

3: $v \leftarrow v_0 * L_{max} / (M - 1)$

4: $x = zeros/(M, 1)$

5: **for** $t = 1$ to $(M - 1)$ do

6: **if** randn < $p_b * p_s$ then

7: nextDir $\leftarrow 2 \cdot v \cdot e^{-i*(\pi+(\text{randn}-0.5))}$

8: else:

9: nextDir ← 0

10: $dv \leftarrow$ **nextDir** + p_s (p_g $*$ (randn+ $i*$ randn) $* I * x$ [t] $*$ (L_{max} / $(M-1)$)

11: $v \leftarrow v + dv$

12: $v \leftarrow v/abs(v)$ * L_{max} / $(M-1)$

13: $x[t+1] \leftarrow x[t] + v$

14: Kernel ← sub pixel interpolation (x)

15: Blurred image ← conv(Kernel, Img)

16: return Blurred image

3.4.5 Generative adversarial networks

(Goodfellow et al., 2014) first proposed the GANs algorithm as a way to describe the relationship between generator and discriminator networks. As the input, the generator network receives noise and produces a sample. The discriminator network receives a real image and created sample and tries to differentiate them. The purpose of the generator is to trick the discriminator by creating samples that are imperceptible from the real one. The relationship between the generator network G and the discriminator network D is depicted below in equation 3.5.

$$\min_G \max_D \mathop{\mathrm{E}}_{x \sim p_r} [\log(D(x))] + \mathop{\mathrm{E}}_{x' \sim p_g} [\log(1 - D(x'))] \quad (3.5)$$

where p_r is the data distribution and p_g is the model distribution, defined by $x' = G(z),\ z \rightsquigarrow P(z)$, the input z is a simple noise distribution.

i. The Generator Network

The generator network contains 4 samples, 3x3 convolutional layers, a 1x1 convolutional

block, 11 DPN stages and 2 transposed convolution blocks.

The input to the generator is a vector or matrix of random numbers that are used as a seed for image generation. The generator can convert a shape tensor (128, 1, 1) to a (3 x 28 x 28) shape tensor image.

ii. The Discriminator Network

This network initiates the function of the generator network to gather statistical information for the restored image.

Using an image as the input, the discriminator executes a categorization of either real or generated. Specifically the input converts a (3 x 64 x 64) tensor to a (1, 1, 1) tensor.

- **GANs algorithm**

Minibatch stochastic gradient descent training of GANs. The number of steps to apply to the discriminator, k, is a hyperparameter. k=1

for number of training iterations **do**

for k steps **do**

Sample minibatch of m noise samples $\{z^{(1)}, \ldots, z^{(m)}\}$ from noise prior $p_g(z)$.

Sample minibatch of m noise samples $\{x^{(1)}, \ldots, x^{(m)}\}$ from data generating distribution $p_{data}(x)$

Update the discriminator by ascending its stochastic gradient:

$$\Delta_{\emptyset_d} = \frac{1}{m} \sum_{i=0}^{m} [\log D(x^{(i)} + \log(1 - D(G(z^{(i)})))] \quad (3.6)$$

end for

Sample minibatch of m noise samples $\{z^{(1)}, \ldots, z^{(m)}\}$ from noise prior $p_g(z)$.

Update the generator by descending its stochastic gradient:

$$\Delta_{\emptyset_g} = \frac{1}{m} \sum_{i=0}^{m} \log(1 - D(G(z^{(i)}))) \quad (3.7)$$

end for

The gradient-based updates use the standard gradient-based learning rule.

3.5 Loss Functions

The applied loss functions are based on content and adversarial loss formulations (Kupyn et al., 2018) and cross-domain consistency loss (T. Wang et al., 2019) that performed well when combining Canny edge detector and GANs using Deep CNN.

i- The first loss is calculated as follow:

$$L = \underset{\leftrightsquigarrow}{L_{GAN}} + \lambda \cdot \underset{\leftrightsquigarrow}{L_{GAN}} \tag{3.8}$$

where the λ experimentally chosen equals to 100. $\underset{\leftrightsquigarrow}{L_{GAN}}$ is the adversarial loss and $\lambda \cdot \underset{\leftrightsquigarrow}{L_{GAN}}$ is the content loss which both make up the total loss. No condition is needed as there is no need to penalize the discriminator. (Wasserstein GANs) used along as a citric function and loss is calculated as follows:

$$L_{GAN} = \sum_{n=1}^{N} D_{\theta_D}\left(G_{\theta_G}(I_B)\right) \tag{3.9}$$

According to (Kupyn et al., 2018) and as per the experimental results, smooth and blurry images are generated when image deblurring is trained without GANs component convergence.

ii- Cross-domain consistency loss:

Loss of cross-domain continuity as a constrained condition ($i.e., A \rightarrow B \rightarrow A$) used in two processes:

- Forward process: The samples are taken from both domains into content vectors $\{{Z_x}^c, {Z_y}^c\}$ and style vectors $\{{Z_x}^s, {Z_y}^s\}$. Content vector is concatenated from source domain and Canny feature vector combines style representations followed by the translation to develop samples and the other domain (u, v) , where $u \in A, v \in B$.

$$u = G_A\left(Z_y{}^c, Z_x{}^s\right) \quad v = G_B\left(Z_x{}^c, Z_y{}^s\right) \tag{3.10}$$

- Backward process: backward translation is performed for the samples $u \in A, v \in B$. Canny feature vector is concatenated with backward translation content vector. The reconstructed samples of the cross-domain are given as:

$$x' = G_A\left(Z_v{}^c, Z_u{}^s\right) \quad y' = G_B\left(Z_u{}^c, Z_v{}^s\right) \tag{3.11}$$

Once the entire bi-direction translation is complete, it results in the cross-domain reconstructed samples. The cross-domain consistency loss-function is depicted below:

$$L_1{}^{cd}\left(E_A{}^c, E_B{}^c, E_A{}^s, E_B{}^s, G_A, G_B\right)$$
$$= \mathbb{E}_A\left[\left\|G_A\left(E_B{}^c(v), \left(E_A{}^s(u)\right) - x\right\|\right] + \left[\left\|G_B\left(E_A{}^c(u), \left(E_B{}^s(v)\right) - y\right\|\right]\right. \tag{3.12}$$

where $u = G_A\left(E_B{}^c(y)\ , E_A{}^s(x)\right)$, $v = G_B\left(E_A{}^c(x), E_B{}^s(y)\right)$.

3.6 Discussion

Inspired by the first Generative Adversarial Networks (GANs) model (Goodfellow et al., 2014), several GANs models improvement optimizations by researchers to accomplish efficient blind image deblurring tasks, and have acquired satisfying results (Kupyn et al., 2018; Xiaonan Zhang et al., 2019). However, the edge-preserving task during the deblurring process remains challenging. This is due to the fact that edges transfer important information about images and are a crucial aspect impacting the visual outcome. Finding a filter to first detect and enhance the edges during the deblurring process is desperately needed. But in terms of image smoothing and adaptability, the conventional Canny edge detection operator is still inadequate. However, taking the improved Gaussian filter into consideration, the adaptive parameters for local image variance and minimum variance to make the edge detection (T. Wang et al., 2019) and smoothing adequate when combined with GANs using CNN in the deblurring process,

would be an effective solution. Thus, the research study proposes combining Canny edge detector filter + Generative Adversarial Networks (GANs) to recover a blind motion image with more focus on edge-preserving derived from a thorough study of these two techniques. The methodology is comprised of a Canny edge detector + generator and discriminator with a trio path neural network.

3.7 Summary

This chapter explained the full methodology of the proposed blind motion image deblurring using Canny edge detector with generative adversarial networks scheme. First, the analysis of the research requirements was described, followed by a brief description of the research design and implementation procedure. The proposed method consists of combining Canny edge detector filter + GANs to recover a m,blind motion image with edge-preserving. The method structure comprises a Canny edge detector + generator and discriminator with a trio path network. This chapter also discussed the general structure of the proposed algorithm and the complete research design and implementation.

CHAPTER 4: EXPERIMENTAL RESULTS AND EVALUATION

4.1 Introduction

A series of experimental results conducted using the dataset described in chapter 3, are presented in this chapter. At the same time, in this chapter, the results of the proposed method will be compared to other traditional BID algorithms. The results of the combined method of Canny edge detector with generative adversarial networks using deep CNN for blind motion image deblurring are presented and compared with other relevant BID that use the same GoPro dataset with a special focus on edge-preserving.

4.2 Experimental environment

The deep learning framework PyTorch was used to develop the experimental model. A Nvidia GeForce GTX GPU hosted the training using the GoPro dataset. 100 GoPro images were reduced in scale by a factor of two and were randomly cropped and sized in dimensions of 256X256. This model is fully convolutional and can be widely applied to images of any size due to its extension training using image patches. Following the method proposed by (Kupyn et al., 2018) 5 gradient descent steps were able to optimize the performance on all 3 channel networks (Canny edge detector + generator and discriminator) using Adam (optimizer). The Adam optimizer with stochastic gradient descent (SGD) is essential for training the loss function and is comprised of content, adversarial and cross-domain consistency loss. The optimal batch size was chosen for network processing in order to fit the GPU RAM. The learning rate of the networks is set to 1/10000 with 300 epochs.

4.3 Objective Evaluation Criteria and Image Quality Measures (IQMs)

To measure the effectiveness of individual schemes or the robustness of image processing and computer vision algorithms, BID quality measures have been established. Previously, the performance measures were adopted from signal processing researchers and as a result these BID schemes were highly prone to errors (Rafael Gonzalez. , 2018). Normally the error is computed using an original and deblurred image pair for a quantitative analysis. High quality is determined by referencing the original image. Many efforts have been made in the past decade in support of image quality measures (IQMs) (Zhou Wang & Bovik, 2002). The process of error measurement requires that the original and the observed images to immobile with respect to each other.

There is lack of a strong comparison base to assess the effectiveness of competing algorithms in the field of image restoration. The majority of image restoration performance quality measures are adapted from various error-based measures such as MSE, SNR and PSNR. Thus, a robust assessment of competing algorithms exclusively for images has been impeded (Zhou Wang & Bovik, 2002).

There are two main categories of IQMs: non-reference and full-reference quality measures. A full-reference IQM requires the original image. In contrast, nonreference IQM is able to assess image quality by directly evaluating its attributes.

4.3.1 Peak Signal to Noise Ratio (PSNR)

Evaluating deblurred image quality necessitates a measure. MSE is a very commonly employed quantitative measure in image processing community (Rafael Gonzalez. , 2018). The MSE between two images f and g is given by,

$$MSE = \frac{1}{MN} \left(\sum_{m=1}^{N} \sum_{n=1}^{M} (I_S(m,n) - I_B(m,n))^2\right) \quad (4.1)$$

PSNR provides quantitative image quality results by using the image range as a way to scale the MSE. The pixel intensity range for grayscale images runs from 0 to 255. The PSNR is measured in decibels (dBs) and is defined using the formula below:

$$PSNR = 10\ log_{10}\ \left(\frac{\sum_{m=1}^{N} \sum_{n=1}^{M} (I_S(m,n) - I_B(m,n))^2}{255^2}\right) dB \quad (4.2)$$

The higher the value of $PSNR$ obtained, the stronger the image quality. The main drawback of measuring the $PSNR$ is that only an estimate of a signal strength for the image is obtainable. While $PSNR$ is effective for measuring different restoration results, it is much less conducive for different images. For example, an image with 15 $dB\ PSNR$ may appear to have stronger quality than an image with 20 $dB\ PSNR$. The results of the proposed method are illustrated in Table 4.1.

4.3.2 Mean Structural Similarity Index (MSSIM)

Structural Similarity ($MSSIM$) score is an objective image quality metric (Z. Wang, Bovik, Sheikh, & Simoncelli, 2004). Assuming two images I_S and I_B, the $MSSIM$ is a function of the luminance $l(I_S, I_B)$, contrast $c(I_S, I_B)$ and structural similarity $s(I_S, I_B)$ of the images.

$$S(I_S, I_B) = t(l(I_S, I_B), c(I_S, I_B)\ s(I_S, I_B)) \quad (4.3)$$

$$l(I_S, I_B) = \frac{2\mu_{I_S}\mu_{I_B} + c_1}{\mu_{I_S}^2 + \mu_{I_B}^2 + c_1} \quad (4.4)$$

$$c(I_S, I_B) = \frac{2\sigma_{I_S}\sigma_{I_B} + c_2}{\sigma_{I_S}^2 + \sigma_{I_B}^2 + c_2} \quad (4.5)$$

$$s(I_S, I_B) = \frac{\sigma_{I_S I_B} + c_3}{\sigma_{I_S}\ \sigma_{I_B} + c_3} \quad (4.6)$$

where μ is the mean, σ is the standard deviation of the image signal and c_1, c_2, c_3 are constants. SSIM has been successfully used for denoising and classification (Gao, Rehman, & Wang, 2011; Rehman & Wang, 2011; L. Zhang, Sheng, & Cha, 2017). A higher value of MSSIM represents an image of high quality. Table 4.1 illustrates the SSIM results of the proposed method. The higher value of SSIM represents a better perceptual quality of an image.

4.3.3 Universal Quality Index (UQI)

Universal Quality Index (UQI) is based on quality perception analyses of correlation, contrast distortion and luminance, of two images. The UQI for two image signals I_S, and I_B is defined in equation 4.6 as,

$$Q(I_S, I_B) = \frac{4\sigma_{I_S I_B}\mu_{I_S}\mu_{I_B}}{(\sigma_{I_S}^2+\sigma_{I_B}^2)(\mu_{I_S}^2+\mu_{I_B}^2)} \tag{4.7}$$

Rearranging equation 4.7, the following equation 4.8 is obtained:

$$Q(I_S, I_B) = \frac{\sigma_{I_S I_B}}{\sigma_{I_S}\sigma_{I_B}} \cdot \frac{2\,\mu_{I_S}\mu_{I_B}}{\mu_{I_S}^2+\mu_{I_B}^2} \cdot \frac{2\,\sigma_{I_S}\sigma_{I_B}}{\sigma_{I_S}^2+\sigma_{I_B}^2} \tag{4.8}$$

The first term measures the correlation coefficient, whereas the second and third terms measure mean luminance and structural similarity. A higher value of UQI represents an image of high quality.

4.3.4 Comparison Metrics

(T. Wang et al., 2019) used comparison metric equation to compute the distance that captures high-frequency information for edge-preserving. The same metric can be used to capture the edge information of the blurred and deblurred images in the research study.

$$L_2 = \frac{1}{2}\,(\sum_{i=1}^{n}\sqrt{(x_i - x)^2}) \tag{4.9}$$

where x_1 represents the generated deblurred image and x represents the original ground truth

$The\ Average\ L_2$ is the distance of every model to the ground truth samples. Table 4.1 illustrates the L_2 results of the proposed method. The lower value of L_2 represents a better perceptual quality of deblurred image related to edge-preserving.

The combination of Canny edge detector with GANs with the edge preserving as the main contribution of proposed method. The detail of the input and the output images of the experiment are shown in Figure 4.1 (a), (b), (c) and (d) respectively.

The results of the proposed method so far are shown in Table 4.4 using the 3 evaluations previously described.

(a)

Input image (blind image)

(b)

Detected edge of the input image

(c)
Detected edge of the restored image

(d)
Restored image

Figure 4.1: The input and the output images of the Canny edge detector + GANs experiment

When only GANs is used, the restored image qualitative and quantitative results are different from when Canny edge detector + GANs combined as per the input and output images in Figure 4.2 (a) and (b). The function loss used for this model.

(a) (b)

Input image (blind image) **Restored image**

Figure 4.2: The input and the output images of the GANs experiment

The results of the proposed method so far are shown in Table 4.1 below using the 3 evaluations previously described.

Table 4.1. Score of results of the proposed method

	PSNR	**SSIM**	**Distance L_2**
Proposed method	**29.5**	**0.9**	**7.7**

Utilization of the cross-domain consistency loss is a primary advantage of this model.

A comparison of the results of the proposed method's experiments with results from existing key studies as shown in Table 4.2. The results of the proposed method demonstrate that the proposed method is more effective than other methods, including a better performance in terms of edge-preserving.

Table 4.2. Performance comparison of the proposed method with existing methods

Methods	PSNR	SSIM	Distance L_2
Image blind deblurring based on Laplacian gradients. Yue Han, J. K. (2018).	29	0.9	9.7
Seungjun Nah, T. H. K., Kyoung Mu Lee. 2017).	26.48	0.807	9.8
Xiaonan Zhang, Y. L., Yunjie Li, Yu Liu, Pengcheng Luo. (2019).	27.98	0.842	9.6
Dong, J., Pan, J., & Su, Z. (2017).	26.50	0.84	9.90
Proposed Method	**29.50**	**0.90**	**7.70**

4.3.5 Analysis

The model is compared not only to the conventional BID algorithms given by Dong et al. (Dong et al., 2017) and Yue Han, J. K (Y. Han & Kan, 2018), but also to the deep-learning utilizing Generative Adversarial Networks (GANs) algorithms proposed by Xiaonan et al. (Xiaonan Zhang et al., 2019) and Seungjun et al. (Nah et al., 2017). PSNR, SSIM and Distance L_2 are chosen as metrics of experimental assessment. Notably, the larger values of PSNR and SSIM metrics are the higher quality of the corresponding images generated, the lower values of Distance L_2 indicator, and the higher quality of corresponding images edges detected. Table

4.2 summarizes the final experimental results. The results show that the proposed method substantially outperforms the other methods listed in Table 4.2. In other words, as compared to these state-of-the-art approaches, the proposed model outperforms them.

4.4 Qualitative and Quantitative Discussion

From Figure 4.1, the output images from the proposed model produce good quality images in terms of PSNR and SSIM measurements. A better quality of edge-preserving is observed due to the comparison metrics equation that computes the distance of the captured high-frequency information for edge-preserving as shown in Table 4.1. The results of the proposed method are compared with the results of other studies in Table 4.2 which illustrate the comparison metrics equation measurement. Combining Canny edge detector with generative adversarial networks results in a better blind motion image deblurring with a focus on edge-preserving. Thus, high frequency information is being preserved when the blurred image's edges are first detected as the input of the proposed model. The GANs networks (generator and discriminator) compete to restore the image and compare it with the sharp one as per Figure 4.1. To this end, the comparison metrics equation used in the experimental results contributes quantitatively. In Table 4.1 and Table 4.2, the $Average\ L_2$ denotes the distance between each model and the sharp images. A low $Average\ L_2$ (7.7) is obtained which is even lower when compared with the results of the other studies.

4.5 Summary

This chapter presented the experimental results of the proposed blind motion image deblurring method that combined Canny edge detector with generative adversarial networks. The results were evaluated PSNR, MSSIM, and the distance L_2. The experimental results are better than those of other traditional BID methods shown in Table 4.2. The proposed method

in this research mainly captures edges of the blurred image and then enhances it to solve the limitations of edge-preserving during BID.

CHAPTER 5: CONCLUSION

This section concludes this research study by demonstrating how the research objectives of this study is achieved, contributions of the study to the field and a brief description of future work.

5.1 Contributions

Digital images have played an important role in the process of acquiring and sharing information in every aspect of human life. They are produced by different digital imaging devices based on specifications and requirements. However, these devices could produce potentially blurred images due to many reasons including camera motion. Camera-motion blur may be caused by camera shake during the exposure time which significantly diminishes quality and leads to blind, blurry, or out-of-focus images. Restoring these images from their degradation (blur) needs image deblurring regularization techniques and robust methods. As a result, image restoration solutions are rendered by either the image deblurring or the blind image deconvolution techniques depending on the restoration problem (prior information) to be solved. The main objective of blind motion image deblurring is to generate a good approximation of the original image from the blurry image. The process is generally called a convolution filtering or deconvolution or deblurring. Many deblurring regularization techniques and methods have been implemented so far including the proposed method of this research. The proposed method entitled blind motion image deblurring using Canny edge detector with generative adversarial networks (GANs).

A blind motion image deblurring with more focus on edge-preserving is described and the combined method of Canny edge detector with generative adversarial networks is introduced, that is optimized using a multi-component loss function. This enabled a kernel-free blind

motion deblurring learning approach compared to traditional mathematical methods. The combined method forms a model of trio networks of a deep CNN that takes the blurred image with its detected edge, enhances it using Canny edge detector as an input, and produces a corresponding detected restored sharp edge with its image, evaluated by the GANs. Then the restored sharp image is compared against the ground truth (sharp) image. The benchmark and evaluation results including PSNR, MSSIM, and the distance $Average\ L_2$ show that the proposed method significantly helps to capture high-frequency information on restored images and detects their preserved edges.

5.2 Conclusion

In this research, blind motion image deblurring using Canny edge detector with generative adversarial networks is analyzed in depth. Combining Canny edge detector with GANs helps improve the edge-preserving treatment during the deblurring process. Canny edge detector helps in the deblurring process to detect the edges of the blurred images, enhance them, and pass them along to GANs. Importantly, this combination method of Canny edge detector + generative adversarial networks incorporate a kernel-free blind motion deblurring learning approach in which a realistic synthetic motion blur enables reproduction of different blur sources. In order to help the generator network, create sharper images, the model include the edge detail which are as a result of Canny edge detector. The experimental results show that the combined method has better performance in deblurring the images and particularly with special treatment in edge-preserving in comparison to other studies referenced in this research.

5.3 Future work

This research study mainly investigated the problem of Blind Motion Image Deblurring. Though good results were achieved in terms of edge-preserving from the proposed scheme which consists of combining Canny Edge Detector + Generative Adversarial Networks (GANs), future work should explore further combination capabilities. However, due to some unexplained causes, there were a few images with pure white background which appear throughout the deblurring process. Some changes are needed in future research to make improvements to explore and develop more efficient loss functions. Some research methods that are outside the scope of this study are recommended below:

- In terms of extending this research work, new learning algorithms may be investigated for the proposed method with a focus on optimization and a faster convergence rate.
- Currently, the proposed method is applicable to blind motion blur however, as the algorithm is quite adaptive, it may easily be tailored to handle other types of blurs by keeping the same edge-preserving techniques applied during the deblurring process.
- Additionally, segmented image deblurring applications, such as a moving object on a stationary background or a centered object on a non-focused background, may be constructed using a variation of the current schemes.

REFERENCES

Ates, H. F. (2019). Deep Learning for Inverse Problems in Imaging. *2019 Ninth International Conference on Image Processing Theory, Tools and Applications (IPTA)*. doi:10.1109/IPTA.2019.8936102

Ayers, G. R., & Dainty, C. C. (1988). Iterative Blind Deconvolution Method and Its Applications. *Optics Section, Blackett Laboratory, Imperial College, London SW7 2BZ, UK, 13, No. 7*. doi:10.1364/OL.13.000547

Babak Rohani, Yigit Yazicioglu, Mehmet Mutlu, Orkun Ogucu, Emre Akgul, & Saranli, A. (2014). Lagrangian based mathematical modeling and experimental validation of a

planar stabilized platform for mobile systems. *Journal of Computational and Applied Mathematics, 259, Part B*, 955-964.

Bagal, M. A. P. T. a. P. S. B. (2015). A Distributed Canny Edge Detector Comparative Appproach.

Bai, Y., Cheung, G., Liu, X., & Gao, W. (2019). Graph-Based Blind Image Deblurring From a Single Photograph. *Ieee Transactions on Image Processing, 28*(3), 1404-1418. doi:10.1109/tip.2018.2874290

Biemond, J., Reginald L. Lagendijk, & Mersereau, R. M. (1990). Iterative Methods for Image Deblurring. *Proceedings of the IEEE, 78*(5), 856 - 883. doi:10.1109/5.53403

Chakrabarti, A. (2016). A Neural Approach to Blind Motion Deblurring. *European Conference on Computer Vision*, 221-235. doi:10.1007/978-3-319-46487-9_14

Chan, T. F., & Wong, C.-K. (1998). Total variation blind deconvolution. *Ieee Transactions on Image Processing, 7*, 370 - 375. doi:10.1109/83.661187

Chang, C.-F., Wu, J.-L., & Tsai, T.-Y. (2017). A Single Image Deblurring Algorithm for Nonuniform Motion Blur Using Uniform Defocus Map Estimation. *Mathematical Problems in Engineering, 2017*, 1-14. doi:10.1155/2017/6089650

Chokshi, R., Israni, D., & Chavda, N. (2016). An Efficient Deconvolution Technique by Identification and Estimation of Blur. *IEEE International Conference on Electronics Information and Communications Technology, pp. 17-23, 2016*. doi:10.1109/RTEICT.2016.7807773

Dong, J., Pan, J., & Su, Z. (2017). Blur kernel estimation via salient edges and low rank prior for blind image deblurring. *Signal Processing: Image Communication, 58*, 134-145. doi:10.1016/j.image.2017.07.004

El-Henawy, M., Amin, A. E., Ahmed, K., & Adel, H. (2018). A Comparative Study On Image Deblurring Techniques. *International Journal of Advances in Computer Science and Technology, 3*(12), 01-08.

Elmi Sola, Y., Zargari, F., & Rahmani, A. M. (2018). Blind image deblurring based on multi-resolution ringing removal. *Signal Processing, 154*, 250-259. doi:10.1016/j.sigpro.2018.09.015

Estrela, V. V., Magalhaes, H. A., & Saotome, O. (2016). Total Variation Applications in Computer Vision. *Kamila NK (ed) Handbook of research on emerging perspectives in intelligent pattern recognition, analysis, and image processing*. doi:10.4018/978-1-4666-8654-0.ch002

Gao, Y., Rehman, A., & Wang, Z. (2011). CW-SSIM Based Image Classification. *2011 18th IEEE International Conference on Image Processing*. doi:10.1109/ICIP.2011.6115659

Goodfellow, I. J., Pouget-Abadie, J., Mirza, M., Xu, B., Warde-Farley, D., Ozair, S., . . . Bengio, Y. (2014). Generative Adversarial Nets. *NIPS'14: Proceedings of the 27th*

International Conference on Neural Information Processing Systems, 3, 2672–2680. doi:10.1145/3422622

Gultekin, G. K., & Saranli, A. (2019). Feature Detection Performance Based Benchmarking of Motion Deblurring Methods: Applications to Vision for Legged Robots. *Image and Vision Computing, 82*, 26-38. doi:10.1016/j.imavis.2019.01.002

Han, & Kan. (2019). Blind Image Deblurring Based on Local Edges Selection. *Applied Sciences, 9*(16). doi:10.3390/app9163274

Han, Y., & Kan, J. (2018). Image blind deblurring based on Laplacian gradients. *Internation Journal of Circuits, Systems and Signal Processing, 12*(26), 173-180.

Hanika, J., Dammertz, H., & Lensch, H. (2011). Edge-Optimized À-Trous Wavelets for Local Contrast Enhancement with Robust Denoising. *Computer Graphics Forum, 30*(7), 1879-1886. doi:10.1111/j.1467-8659.2011.02054.x

He, K., Zhang, X., Ren, S., & Sun, J. (2015). Deep Residual Learning for Image Recognition. *2016 IEEE Conference on Computer Vision and Pattern Recognition (CVPR)*. doi:10.1109/CVPR.2016.90

Khan, A. (2014). Efficient Methodologies for SingleImage Blind Deconvolution and Deblurring. *The University of Manchester (United Kingdom), ProQuest Dissertations Publishing, 2014. 10030610*.

Krishnat B. Pawar, S. L. N. (2016). Distributed Canny Edge Detection Algorithm Using Morphological filter. *IEEE International Conference On Recent Trends In Electronics Information Communication Technology, May 20-21, 2016, India*. doi:10.1109/RTEICT.2016.7808087

Kupyn, O., Budzan, V., Mykhailych, M., Mishkin, D., & Matas, J. (2018). DeblurGAN: Blind Motion Deblurring Using Conditional Adversarial Networks. *2018 IEEE/CVF Conference on Computer Vision and Pattern Recognition*. doi:10.1109/CVPR.2018.00854

Lagendijk, R. L., & Biemond, J. (2009). Chapter 14 - Basic Methods for Image Restoration and Identification. *The Essential Guide to Image Processing (Second Edition)*(2005), 323-348. doi:10.1016/B978-012119792-6/50074-7

Lagendijk, R. L., Biemond, J., & Boekee, D. E. (1988). Regularized Iterative Image Restoration with Ringing Reduction. *IEEE Transactions on Acoustics Speech and Signal Processing, 36*(12), 1874 - 1888. doi:10.1109/29.9032

Levin, A., Weiss, Y., Durand, F., & Freeman, W. T. (2011). Efficient Marginal Likelihood Optimization in Blind Deconvolution. *CVPR 2011*. doi:10.1109/CVPR.2011.5995308

Lucas, A., Iliadis, M., Molina, R., & Katsaggelos, A. K. (2018). Using Deep Neural Networks for Inverse Problems in Imaging: Beyond Analytical Methods. *IEEE Signal Processing Magazine, 35*(1), 20-36. doi:10.1109/msp.2017.2760358

Lucy, L. B. (1974). An iterative technique for the rectification of observed distributions. *The Astronomical Journal, 79*(6), 745-749.

Mane, M. A. S., & Pawar, P. M. M. M. (2014). Removing Blurring From Degraded Image Using Blind Deconvolution with Canny Edge Detection Technique. *International Journal of Innovative Research in Advanced Engineering (IJIRAE) ISSN: 2349-2163, 1*(11).

Nah, S., Kim, T. H., & Lee, K. M. (2017). Deep Multi-scale Convolutional Neural Network for Dynamic Scene Deblurring. *IEEE Conference on Computer Vision and Pattern Recognition (CVPR)*. doi:10.1109/CVPR.2017.35

Pan, J., Sun, D., Pfister, H., & Yang, M.-H. (2016, 2016). *Blind Image Deblurring Using Dark Channel Prior*. Paper presented at the 2016 IEEE Conference on Computer Vision and Pattern Recognition (CVPR).

Pandey, A., & Gregory, J. (2018). Iterative Blind Deconvolution Algorithm for Deblurring a Single PSP/TSP Image of Rotating Surfaces. *Sensors, 18*(9), 3075. doi:10.3390/s18093075

Perrone, D., & Favaro, P. (2016). A Clearer Picture of Total Variation Blind Deconvolution. *IEEE Transactions on Pattern Analysis and Machine Intelligence, 38*(6), 1041-1055. doi:10.1109/tpami.2015.2477819

Preeti Topno, G. M. (2019). An Improved Edge Detection Method based on Meidan filter. *2019 Devices for Integrated Circuit (DevIC)*. doi:10.1109/DEVIC.2019.8783450

Rafael Gonzalez. , W. R. (2018). Digital Image Processing, 4th Edition. *Pearson*.

Rehman, A., & Wang, Z. (2011). SSIM-based non-local means image denoising. *2011 18th IEEE International Conference on Image Processing*. doi:10.1109/ICIP.2011.6116065

Richardson, W. H. (1972). Bayesian-Based Iterative Method of Image Restoration. *Journal of Optical Society of America, 62*(1), 55-59. doi:10.1364/JOSA.62.000055

Ruiz, P., Zhou, X., Mateos, J., Molina, R., & Katsaggelos, A. K. (2015). Variational Bayesian Blind Image Deconvolution: A review. *Digital Signal Processing, 47*, 116-127. doi:10.1016/j.dsp.2015.04.012

Ruomei, Y., & Ling, S. (2016). Blind Image Blur Estimation via Deep Learning. *IEEE Trans Image Process, 25*(4), 1910-1921. doi:10.1109/TIP.2016.2535273

Sada, M. M., & Goyani, M. M. (2018). Image Deblurring Techniques: A Detail Review. *International Journal of Scientific Research in Science, Engineering and Technology, 4*, 176-188. doi:10.32628/IJSRSET184230

Sorel, M., & Flusser, J. (2008). Space-Variant Restoration of Images Degraded by Camera Motion Blur. *Ieee Transactions on Image Processing, 17*(2), 105-116. doi:10.1109/tip.2007.912928

Stockham, C., R.B. Ingebretsen. (1975). Blind Deconvolution Through Digital Signal Processing. *Proceedings of the IEEE, 63*(4), 678-692. doi:10.1109/PROC.1975.9800

Su, Z., Zeng, B., Miao, J., Luo, X., Yin, B., & Chen, Q. (2018). Relative reductive structure-aware regression filter. *Journal of Computational and Applied Mathematics, 329*, 244-255. doi:10.1016/j.cam.2017.05.047

Thombare, M. A. P., & Bagal, P. S. B. (2015). A Distributed Canny Edge Detector Comparative Appproach. *2015 International Conference on Information Processing (ICIP) Vishwakarma Institute of Technology. Dec 16-19, 2015*.

Thongkor, K., Supasirisun, P., & Amornraksa, T. (2015). Digital Image Watermarking based on Regularized Filter. *14th International Association of Pattern Recognition International Conference on Machine Vision Applications*, 493-496.

Ulyanov, D., Vedaldi, A., & Lempitsky, V. (2018). Deep Image Prior. *2018 IEEE/CVF Conference on Computer Vision and Pattern Recognition*. doi:10.1109/cvpr.2018.00984

Wang, J., Lu, K., Wang, Q., & Jia, J. (2012). Kernel Optimization for Blind Motion Deblurring with Image Edge Prior. *Mathematical Problems in Engineering, 2012*, 1-10. doi:10.1155/2012/639824

Wang, T., Zhang, T., Liu, L., Wiliem, A., & Lovell, B. (2019). CANNYGAN Edge-Preserving Image Translation with Disentangled Features. *2019 IEEE International Conference on Image Processing (ICIP)*. doi:10.1109/ICIP.2019.8803828

Wang, Z., & Bovik, A. C. (2002). A Universal Image Quality Index. *IEEE Signal Processing Letters, 9*(3), 81 - 84. doi:10.1109/97.995823

Wang, Z., Bovik, A. C., Sheikh, H. R., & Simoncelli, E. P. (2004). Image quality assessment: from error visibility to structural similarity. *IEEE Trans Image Process, 13*(4), 600-612. doi:10.1109/tip.2003.819861

Xiangyu, X., Jinshan, P., Yu-Jin, Z., & Ming-Hsuan, Y. (2018). Motion Blur Kernel Estimation via Deep Learning. *Ieee Transactions on Image Processing, 27*(1), 194-205. doi:10.1109/TIP.2017.2753658

Xu, L., Ren, J. S., Liu, C., & Jia, J. (2015). Deep Convolutional Neural Network for Image Deconvolution. *Advances in Neural Information Processing Systems 27 (NIPS 2014)*, 1790–1798.

Xu, L., Zheng, S., & Jia, J. (2013). *Unnatural L0 Sparse Representation for Natural Image Deblurring*. Paper presented at the 2013 IEEE Conference on Computer Vision and Pattern Recognition, Portland, OR, USA.

Yang, D., & Qin, S. (2016). Restoration of Partial Blurred Image Based on Blur Detection and Classification. *Journal of Electrical and Computer Engineering, 2016*, 1-12. doi:10.1155/2016/2374926

Yuan, L., & Xu, X. (2015). *Adaptive Image Edge Detection Algorithm Based on Canny Operator*. Paper presented at the 2015 4th International Conference on Advanced Information Technology and Sensor Application (AITS).

Zeng, Z., Yu, Y. K., & Wong, K. H. (2018). Adversarial Network for edge detection. *2018 Joint 7th International Conference on Informatics, Electronics & Vision (ICIEV) and 2018 2nd International Conference on Imaging, Vision & Pattern Recognition (icIVPR)*. doi:10.1109/ICIEV.2018.8641005

Zhang, H., Li, Y., Wu, Y., & Zhang, Z. (2020). BID: An Effective Blind Image Deblurring Scheme to Estimate the Blur Kernel for Various Scenarios. *IEEE Access, 8*, 9185-9195. doi:10.1109/access.2020.2964621

Zhang, L., Sheng, Y., & Cha, L. (2017). SSIM-based optimal non-local means image denoising with improved weighted Kernel function. *2017 36th Chinese Control Conference (CCC)*. doi:10.23919/ChiCC.2017.8028216

Zhang, X., Lv, Y., Li, Y., Liu, Y., & Luo, P. (2019). A Modified Image Processing Method for Deblurring based on GANs Networks. *2019 5th International Conference on Big Data and Information Analytics (BigDIA)*, 29-33. doi:10.1109/BigDIA.2019.8802800

Zhang, X., Wang, R., Jiang, X., Wang, W., & Gao, W. (2016). Spatially variant defocus blur map estimation and deblurring from a single image. *Journal of Visual Communication and Image Representation, 35*, 257-264. doi:10.1016/j.jvcir.2016.01.002